Effect of bubble volume fraction on the shear and extensional rheology of bubbly liquids based on guar gum (a Giesekus fluid) as continuous phase

M.D. Torres[a,b], B. Hallmark[a] and D.I. Wilson[a]

[a]Department of Chemical Engineering and Biotechnology, New Museums Site, University of Cambridge, Pembroke St, Cambridge, CB2 3RA, UK.

[b]Department of Chemical Engineering, University of Santiago de Compostela, Lope Gómez de Marzoa St, Santiago de Compostela, E-15782, Spain.

Submitted to

Journal of Food Engineering

September 2014

Revised manuscript

Corresponding author

Dr Bart Hallmark

Tel: +44 1223 762783

E-mail: bh206@cam.ac.uk

Post Department of Chemical Engineering and Biotechnology, New Museums Site, University of Cambridge, Pembroke St, Cambridge, CB2 3RA, UK.

Effect of bubble volume fraction on the shear and extensional rheology of bubbly liquids based on guar gum (a Giesekus fluid) as continuous phase

M.D. Torres · B. Hallmark · D.I. Wilson

Abstract

The effect of air bubble volume fraction, ϕ, on the steady shear and extensional rheology of aqueous guar gum solutions was studied at $0 \leq \phi \leq 0.25$ and gum concentrations of (*i*) 5 g/L and (*ii*) 10 g/L, corresponding to solutions in the (*i*) semi-dilute and (*ii*) entanglement regime. The rheological response of the fluids was largely independent of bubble size but strongly dependent on ϕ. The viscous and elastic moduli increased with increasing bubble volume fraction, with elastic dominance prevalent at the higher gum concentration. Extensional rheometry, investigated using filament stretching, revealed that the thinning dynamics of the liquid thread were affected by bubble size, but the filament rupture time was primarily dependent on ϕ. The rheological behaviour in both shear and extension could be modelled as a single mode Giesekus fluid, with a single set of parameters able to describe both the shear and extensional behaviour in the semi-dilute regime. In the entanglement regime the single mode Giesekus fluid could fit the shear data or the extensional data individually, but not both. The fitted Giesekus fluid model parameters exhibited a strong dependency on ϕ, offering a way to predict the flow behaviour of these complex food fluids.

Keywords Extensional; Foams, Non-ionic hydrocolloids; Relaxation time; Viscoelasticity

M.D. Torres
Department of Chemical Engineering, University of Santiago de Compostela, Lope Gómez de Marzoa St, Santiago de Compostela, E-15782, Spain.

B. Hallmark (✉) E-mail address: bh206@cam.ac.uk
Department of Chemical Engineering and Biotechnology, New Museums Site, University of Cambridge, Pembroke St, Cambridge, CB2 3RA, UK.

D.I. Wilson
Department of Chemical Engineering and Biotechnology, New Museums Site, University of Cambridge, Pembroke St, Cambridge, CB2 3RA, UK.

Nomenclature

Roman

A	dimensionless group defined in Equation [19], -
a	Giesekus mobility parameter, -
Bo	Bond number, -
Ca	Capillary number, -
c^*	critical concentration, g/L
D	filament diameter (µm)
D_{mid}	diameter of the filament at midpoint (µm)
D_0	initial sample diameter (µm)
D_1	diameter of the filament when first formed (µm)
d_{max}	largest measured bubble diameter, m
d_{min}	smallest measured bubble diameter, m
d_n	Needle diameter, m
k	time constant, s^{1-n}
g	gravitational constant, m/s^2
G'	storage modulus, Pa
G''	loss modulus, Pa
M_n	number average molecular weight, g/mol
M_w	weight average molar mass, g/mol
M_z	higher average molecular weight, g/mol
n	flow index, -
n_b	number of bubbles, -
n_2	parameter in shear expression
N_c	number of classes of bubbles, -
p	probability, -
Q	volumetric flow of fluid within needle, m^3/s
R_{pp}	radius of parallel plate geometry, m

R^2	square of the correlation coefficient, -
t	time, ms
t_{cap}	capillary time, s
t_F	time to capillary break-up, ms
T	torque, N m
w	class interval width, m
X	filament shape factor, Equation (9), -

49

Greek

α	surface tension between liquid phase and the air, N/m
ε	Hencky strain, -
$\dot{\varepsilon}$	Hencky strain rate, s^{-1}
ϕ	air volume fraction, -
$\dot{\gamma}$	shear rate, s^{-1}
$\dot{\gamma}_R$	shear rate experienced at the rim of the parallel plates, s^{-1}
η_{app}	apparent viscosity, Pa s
η_e	estimated apparent extensional viscosity, Pa s
η_0	zero-shear-rate viscosity, Pa s
η_{r0}	relative viscosity at low shear rate, -
η_r	relative viscosity, -
η_∞	infinite shear rate viscosity, Pa s
Λ	group used within shear expression
λ	relaxation time, ms
μ	mean, μm
ρ	density, kg m^{-3}
ρ_s	density of aerated sample, kg m^{-3}
ρ_{us}	density of de-aerated sample, kg m^{-3}
σ	standard deviation

Introduction

Bubbly liquids are dispersions of bubbles in a liquid, with bubble volume fractions typically ranging up to 50%. The continuous liquid phase is usually viscous, retarding coalescence and creaming. In the food sector, the bubble phase is usually air and aerated liquid foods are ubiquitous, from beverages to baked products, ice creams, dairy systems and confectionery, *e.g*. van Aken (2001). Aeration yields a softer texture, increased spreadability, a more homogeneous appearance and a more uniform distribution of taste (Thakur *et al.*, 2003). Moreover, air cells can be used to replace fats in low-calorie products and healthier foods (Gabriele *et al*., 2012). Bubbly liquids are also encountered in nature in the form of magmas (Manga and Loewenberg, 2001; Gonnermann and Manga, 2007) and in other industrial sectors in the form of foamed cement (Ahmed *et al*., 2009), extracted crude oil (Abivin *et al*., 2009), cosmetics and personal care products (Malysa and Lunkenheimer, 2008).

It is important to understand the rheology of these aerated materials in order to develop and improve manufacturing routes. The presence of the bubble phase modifies the behaviour of the liquid, giving rise to shear-thinning and viscoelastic behaviour (Llewellin *et al*., 2002; Torres *et al*., 2013). In steady shear, at low shear rates the bubbles resist deformation and the behaviour resembles that of suspensions, with relative viscosity increasing with bubble volume fraction, ϕ. At higher shear rates, bubble deformation occurs, promoting alignment with the flow and giving rise to shear-thinning. The transition to shear-thinning behaviour in bubbly liquids is usually discussed with reference to the capillary number, *Ca*, which compares the deforming stress arising from fluid shear to the restoring capillary pressure (Rust and Manga, 2002). However, other workers that have studied emulsions (e.g. Golemanov *et al*., 2008) have demonstrated that *Ca* is not a reliable indicator of the transition in densely populated systems as the shear stress acting on the dispersed phase in high volume fraction systems will differ noticeably from that in the continuous phase alone owing to bubble/droplet crowding effects. Llewellin *et al*. (2002) provided a good review of the pertinent literature as part of their work presenting a model for bubbly liquid rheology under steady and oscillatory shear conditions.

Most of studies on bubbly liquids in food and other applications have considered systems where the liquid phase is Newtonian (*e.g.* Thompson *et al*., 2001; Llewellin *et al*., 2002; Rust and Manga, 2002). Many bubbly liquids used in food manufacture feature non-Newtonian solutions or suspensions as the continuous phase. Examples include cake batters, and whipped creams and shortenings prepared by incorporating significant volumes of air into a viscous hydrocolloid matrix. Several natural water-soluble polymers, such as guar gum, are in widespread use in the food industry. The presence of a significant number of bubbles renders them strongly visco-elastic (Torres *et al*., 2013) and the existing theoretical treatments for bubbly liquids are not able to describe such materials. Similar findings were reported for cake batters (Meza *et al*., 2011; Chesterton *et al*., 2011a).

Food processing operations expose bubbly liquids to steady shear and extensional flow, and being able to predict behaviour in both modes is important for design and formulation of new food products. Experimental investigation of extensional flows is challenging, particularly for viscoelastic materials (Vadillo *et al*., 2012), partly due to difficulties in creating a purely extensional flow. Much of the work on extensional rheology has considered well characterised, model synthetic polymer solutions, and there is little published on the behaviour of systems containing guar gum and its derivatives, besides that by Tatham *et al*. (1995), Duxenneuner *et al*. (2008) and Bourbon *et al*. (2010) over a narrow range of concentrations (0.39-0.97 g/L) using a capillary breakup extensional rheometer (CaBER) device. Torres *et al*. (2014a) presented measurements of the extensional rheology of unaerated guar gum solutions obtained using the Cambridge Trimaster filament stretching device (Vadillo *et al.*, 2010) over a wider range of concentrations (1-20 g/L), crossing the transition from the dilute to the entangled regime. To our knowledge, the effect of air volume fraction on the extensional properties of bubbly liquids prepared with guar gum or similar biopolymers has not been reported previously. This paper reports a systematic investigation of the effect of bubble volume fraction on the shear and extensional behaviour of aerated bubbly liquids with guar gum solutions as the continuous phase. Two guar gum concentrations are considered: one exhibiting semi-dilute behaviour, and another giving solutions in the entanglement regime.

Many mathematical treatments of extensional behaviour have been derived (Bird *et al*., 1987; Larson, 1988). Most testing has been conducted with shear flows, and the reliability of these equations for strongly extensional flows, where a substantial degree of stretching is anticipated, is not well understood (Gupta *et al*., 2000). In a companion paper (Torres *et al.,* 2014b), we demonstrated that the Giesekus constitutive equation (Giesekus, 1982), which was originally developed to describe the shear behaviour of polymer solutions, can provide a good description of the shear and extensional rheology of unaerated aqueous guar gum solutions in the semi-dilute regime. That study suggested that simple shear tests could be used to give a reliable estimate of extensional behaviour for Giesekus fluids when a common set of parameters describe both types of flow.

The particular aim of this work is to extend the current framework for understanding the behaviour of bubbly liquids prepared with a non-Newtonian liquid phase to include their extensional rheology. The influence of ϕ on steady shear, oscillatory shear and extensional shear of bubbly liquids prepared with aqueous guar gum solutions was investigated experimentally. Bubble size distributions were modified by syringing. The single mode Giesekus fluid model, which describes the rheology of the unaerated solutions well, is shown to provide a reasonable description of these aerated systems with $\phi \leq 0.25$. The effect of ϕ on the Geisekus fluid parameters is presented, in analogy to studies of solids volume fraction on suspension behaviour.

Materials and Methods

Raw materials

Commercial guar gum was supplied by Sigma-Aldrich (batch no. 041M0058V, India) with a molecular weight, $M_{w,}$ of 3.0×10^6 g/mol and a small degree of polydispersity, characterised by $M_w/M_n = 1.13$ and $M_z/M_n = 5.15$, where M_n and M_z are the number average molecular weight and higher average molecular weight, respectively.

Sample preparation

Aqueous solutions of guar gum (5 and 10 g/L) were prepared following the procedure reported by Torres *et al*. (2013). The polymer was dispersed in tap water by stirring at 1400 rpm on a magnetic hotplate stirrer (VMS-C4 Advanced, VWR, UK) at room temperature overnight to ensure complete hydration of the gum. Some air was incorporated into the solution during stirring and deaerated samples of the continuous phase were obtained by centrifugation at 2250 rpm for 5 min. Aeration of guar gum solutions was carried out in a planetary-action mixer (Hobart N50-110, Hobart UK, London). Details of this mixer and the wall shear rates generated are reported in Chesterton *et al*. (2011b). The liquids were whisked for 1 to 10 minutes at a speed setting of 3, giving estimated wall shear rates of 500 s^{-1}. The air volume fraction increased with time, reaching $\phi \approx 0.25$ after 10 min.

Samples with smaller bubble sizes were obtained by pumping a fraction of each whisked sample from a syringe (barrel i.d. 22 mm) through a needle with internal diameter, d_n, of 1 mm. Pumping was performed using a digitally-controlled syringe pump (Cole Parmer, UK). The apparent wall shear rate in the needle was estimated from $32Q/\pi d_n^3$ as 225 s^{-1}, *i.e*. less than that experienced at the planetary mixer walls. All samples were, at minimum, tested in duplicate.

The air volume fraction, ϕ, was determined gravimetrically following the procedure reported by Allais *et al*. (2006). Measurements were carried out at room temperature using a 150 mL plastic cup. The cup was filled with sample and the surface levelled using a spatula. The cup was then weighed

and the density determined as the ratio of the mass of sample to cup volume. The air volume fraction was calculated from:

$$\phi = 1 - \frac{\rho_s}{\rho_{us}} \quad (1)$$

where ρ_s and ρ_{us} are the densities of aerated and unaerated samples, respectively. Measurements were made at least in triplicate.

Bubble size measurements

Estimates of the bubble size distributions (with and without syringing) were determined quantitatively by static measurements using a Morphologi G3S image analysis system (Malvern Instruments Ltd., UK). Freshly prepared samples were placed between two microscope slides held 1 mm apart by plastic shims in the Morphologi unit and photographed at 10× magnification. Six consecutive and slightly overlapping images were taken, with the total view spanning two photographs in width and three photographs in height. The bubble size distribution was similar in each photograph. This arrangement minimised the number of partially viewed bubbles and maximised the area-to-perimeter ratio. Image processing was done semi-automatically: the diameter of each bubble was traced manually, and image analysis software (Corel Draw X3 Pro) was used to measure the traced lines. The air bubbles were sufficiently dispersed to allow bubble diameters to be traced readily. Allais *et al*. (2006) employed a similar method and suggested a minimum of 250 measurements for accurate representation of an aerated sample. At least 250 bubbles were measured in each sample in this work.

The bubble size data were grouped into classes following the protocol reported by Jakubczyk and Niranjan (2006), where the number of classes, N_c , and the class interval width, w, were given by:

$$N_C = \sqrt{n_b} \quad (2)$$

$$w = \frac{d_{\max} - d_{\min}}{N_C} \quad (3)$$

with n_b being the number of bubbles measured and d_{min} and d_{max} the smallest and largest measured bubble diameters, respectively. The bubble size data were evaluated by radius and were found to follow a log-normal distribution, as reported previously for cake batters by Chesterton *et al.* (2013).

Shear rheology

Shear rheological measurements (under steady and oscillatory shear) were performed at 20°C on a Bohlin CVO120HR controlled-stress rheometer (Malvern Instruments, Malvern, UK) using sand-blasted parallel plates (25 mm diameter and 1 mm gap) to prevent wall slippage. Samples were loaded carefully to ensure minimal structural damage, and held at rest for 5 min before testing to allow stress relaxation and temperature equilibration. A thin film of a Newtonian silicone oil (viscosity 1 Pa s) was applied to the exposed sample edges to prevent evaporation. Initial testing on a series of samples showed little difference between measurements made within 2 hours of sample preparation so all tests were conducted within this time frame. This outcome indicated that any phenomena such as coalescence and ripening which could change the number and size of bubbles were not significant over this period. All measurements were made under isothermal conditions and, at minimum, duplicated. Error bars are plotted where the measurement uncertainty was greater than the symbol size.

Steady shear measurements

Viscous behaviour was investigated using steady shear measurements. The apparent viscosity, η_{app}, was determined as function of shear rate, $\dot{\gamma}$, over the range 0.1 to 1000 s^{-1}. Samples were sheared for 5 s at each shear rate in order to obtain steady-state. Since the shear rate varies with radial position in the parallel plate geometry, the apparent viscosity data were calculated using (Steffe, 1996):

$$\eta_{app}(\dot{\gamma}_R) = \frac{T}{2\pi R_{pp}^3 \dot{\gamma}_R}\left(3 + \frac{d\ln T}{d\ln \dot{\gamma}_R}\right) \quad (4)$$

where $\dot{\gamma}_R$ is the shear rate evaluated at the rim, R_{pp} is the radius of the parallel plates and T is the torque.

The measured shear response of guar gum solutions of varying air volume fraction was fitted to the result for steady state shear of a single mode Giesekus fluid (Giesekus, 1982). The following expressions have been successfully applied to describe the flow curve of aqueous guar gum solutions in the semi-dilute regime (Torres *et al*., 2014b).

$$\eta_{app}(\dot{\gamma}) = \frac{\eta_0(1-n_2)}{1+(1-2a)n_2} + \eta_\infty \tag{5}$$

where the dimensionless terms n_2 and Λ are given by

$$n_2 = \frac{1-\Lambda}{1+(1-2a)\Lambda} \tag{6}$$

$$\Lambda = \sqrt{\frac{\sqrt{1+16a(1-a)\lambda^2\dot{\gamma}^2}-1}{8a(1-a)\lambda^2\dot{\gamma}^2}} \tag{7}$$

with λ being the relaxation time and a the mobility parameter. Several workers (Schleiniger, 1991; Yoo and Choi, 1989) have reported that although the mobility parameter can theoretically take the range $0 < a < 1$, only physically realistic solutions are obtained over the range $0 < a < 0.5$; an upper limit of 0.5 was hence used here.

Oscillatory shear measurements

Viscoelastic behaviour was investigated using small amplitude oscillatory shear testing. Strain sweeps (0.01-10%) were performed at 0.01 and 10 Hz prior to each frequency sweep in order to identify the region of linear viscoelasticity (LVE). Frequency sweeps were performed over the range 0.01 to 10 Hz at a strain amplitude of 1%, well below the LVE limit, from which the storage modulus, *G'*, and loss modulus, *G"* were determined using the rheometer software.

Extensional rheology

Extensional rheology was investigated using the Cambridge Trimaster, a high speed filament stretch and break-up device described by Vadillo *et al*. (2010). The apparatus consists of two cylindrical 1.2 mm diameter stainless steel stubs which are moved vertically apart at high speed with high spatial precision. Measurements reported here featured an initial gap spacing of 0.6 mm, final gap spacing

of 1.5 mm and separation speed of 75 mm s^{-1}. The filament stretching and thinning profiles were monitored using a high speed camera (Photron Fastcam SA3) which allows the diameter of the filament midpoint, $D_{mid}(t)$, to be measured to ±0.1 μm at a rate of 5000 frames per second. All experiments were performed at least in duplicate in an air-conditioned room at 20 °C.

Filament measurements were obtained using automatic image analysis in the Cambridge Trimaster software. Three characteristic diameters were recorded: D_0, the initial sample diameter, being that of the plates; D_1, the diameter of the filament when first formed, and D_b, the diameter at break-up. The symmetry of the sample during thinning was checked by comparing the filament diameter at positions 100 μm above and below the mid-plane. Results obtained from non-symmetric filaments were discarded. The influence of gravity is characterised by the Bond number:

$$Bo = \frac{\rho g D_0^{\,2}}{4\alpha} \tag{8}$$

where g is the gravitational constant and α is the liquid-air surface tension. The sample density was estimated as outlined above: the parameters lie in the range ρ ~ 1090 kg m^{-3}, g = 9.81 m s^{-2}, D_0 = 1.2 mm and α ~ 0.067 N m^{-1}, giving Bo values around 0.04. Gravitational effects were therefore expected to be negligible.

The Trimaster device did not feature a force transducer so separating forces were not recorded. Estimates of the apparent extensional viscosity, η_e, can be obtained from the filament regime using (Vadillo *et al*., 2010):

$$\eta_e = (2X - 1)\frac{-\alpha}{dD_{mid}(t)/dt} \tag{9}$$

where X is a coefficient which accounts for the deviation of the filament shape from a uniform cylinder due to inertia and gravity, α is the surface tension between the liquid phase and the air, and t is the elapsed time. Several authors report X values of ~0.7 for polymer solutions at approximately zero Reynolds number (McKinley and Tripathi, 2000; Vadillo et al., 2010) whereas an X value of 0.5912 was derived by Eggers (1997: further reported by McKinley and Tripathi, 2000) from the universal similarity solution describing the breakup of a Newtonian fluid at non-zero Reynolds

numbers. Although the non-zero Reynolds number condition (an Ohnesorge number ≤ 0.2) can be shown to apply for the solution containing 1 g/L of guar gum, use of X = 0.59 introduces an unphysical discontinuity in the trends of extensional viscosity as a function of concentration, presented later. X values around 0.7 were thus used in evaluating Equation (9).

The equilibrium surface tension between the guar gum solutions and air at 21°C was determined using the sessile drop method with a Kruss Drop Shape Analyser 100 device. Values reported are the mean from at least ten measurements.

The Hencky strain, ε, experienced by the sample at the axial midplane at time t is defined using the midfilament diameter:

$$\varepsilon = 2\ln\left(\frac{D_1}{D_{mid}(t)}\right) \tag{10}$$

Torres *et al*. (2014b) showed that the evolution of the filament mid-plane diameter for a single mode Giesekus fluid undergoing filament stretching for time t is given by

$$(4a-3)\ln\left(\frac{\left(D/D_1\right)+2a\lambda\alpha/D_1\eta_0}{1+2a\lambda\alpha/D_1\eta_0}\right)-\frac{2\eta_0 D_1}{\alpha\lambda}\left(D/D_1-1\right)=\frac{t}{\lambda} \tag{11}$$

where D is the filament diameter and D_1 is its initial value.

The capillary time, t_{cap}, which is the timescale for characterising capillary break-up in viscous Newtonian fluids (Anna and McKinley, 2001), is another characteristic time scale of importance in elasto-capillary thinning studies. The capillary time quantifies the relative effects of capillary and viscous forces,

$$t_{cap} = \frac{\eta_0 D_1}{2\alpha} \tag{12}$$

where D_1 is used instead of D_0 in this study since the initial filament diameter (D_1) varied widely between notionally identical samples. This approach was previously used for cake batters and gave

consistent results (Chesterton *et al*., 2011a). Further details of the apparatus and method are given in Vadillo *et al*. (2010).

Statistical analysis

The parameters of the considered models were determined from the experimental data with a one-factor analysis of variance (ANOVA) using PASW Statistics (v.18, IBM SPSS Statistics, New York, USA). When the analysis of variance indicated differences among means, a Scheffé test was carried out to differentiate between means with 95% confidence ($p < 0.05$).

Results and Discussion

Bubbly size distribution

Bubbly liquids prepared with guar gum at 5 and 10 g/L were aerated for different periods (1, 2, 6 and 10 min) in order to obtain several air volume fractions, ϕ. The guar gum solution contained some bubbles initially ($\phi \sim 0.05$) and ϕ rose from 0.10 to 0.25 as the aeration time was increased from 1 to 10 min. The effect of syringing samples with given ϕ was also studied. Selected images, for $\phi \sim 0.25$ guar gum bubbly liquids aerated for 10 min with and without syringing, are presented in Figure 1. Bubbly liquids aerated for shorter times showed similar microstructures and marginally larger bubbles. Similar observations were reported for cake batters by Chesterton *et al*. (2011b).

Figure 1(*c*) shows the corresponding bubble size distributions obtained from optical microscopy, fitted to a log-normal distribution. The parameters of the log-normal distributions are reported in Table 1. All the bubbly liquids studied, *i.e*. both those prepared with 5 g/L and 10 g/L guar gum solutions, exhibited similarly unimodal size distributions. The increase in ϕ was accompanied by an increase in the number of bubbles and a small decrease in their mean diameter (Table 1). After 10 min aeration, ϕ approached 0.25 and the measured diameters ranged from 20 to 350 μm, with a mode around 80 μm.

Syringing reduced the bubble diameter range to 5-270 μm, with a mode around 30 μm. Figure 1 and Table 1 show that similar trends were observed with 5 and 10 g/L guar gum solutions: syringing yielded distributions with smaller bubbles in all cases. Syringing exposes the bubbles to extensional and linear shear, and the contributions of both are considered next. The apparent shear rate (*i.e*. the wall shear rate for a Newtonian fluid) in the needle was around 250 s^{-1}, which is less than the maximum shear rate estimated at the wall in the mixer (around 500 s^{-1}). The local shear rate in the centre of the needle will be smaller than the above value, and these factors suggest that the larger bubbles are not broken up as they pass along the needle. The capillary number estimated for bubbles with radius 15 μm, using the shear stress measured for the bubbly liquids at the above wall shear rates, was ~ 0.001. This is considerably smaller than the critical value of *Ca* for droplet/bubble breakup on the Grace diagram for droplet breakup (Grace, 1982), although this limit is not strictly valid here owing to the large difference in viscosities and non-Newtonian nature of the continuous phase. The above evidence indicates that the extensional shear experienced by the bubbles at the needle entry is responsible for the reduction in bubble size.

Steady shear measurements

Representative flow curves for centrifuged guar gum solutions prepared at 5 g/L and 10 g/L and the corresponding bubbly liquid generated by 10 min aeration are shown in the form of shear rate sweeps in Figure 2. Similar profiles and magnitudes were found for samples after syringing (data not shown). The guar gum solutions and their bubbly liquids all exhibited shear-thinning behaviour, where the apparent viscosity decreased with shear rate, as reported elsewhere for guar gum solutions (Chenlo *et al*. 2010). The latter workers found that the shear rate at which the zero-shear rate viscosity plateau ended depended on polymer concentration, which is also evident in Figure 2. In all cases, the apparent viscosity at each shear rate increases with air volume fraction, which is consistent with the results previously reported by Torres *et al.* (2013) working with bubbly liquids prepared by whisking air into guar gum solutions at 10 g/L. Similar behaviour was found by Chesterton *et al*. (2012) in their study of cake batters. In both cases, the shear-thinning nature of the continuous phase plays an essential role in giving a high apparent viscosity after bubbles are generated in the mixer, retarding subsequent creaming of the bubbles in the system.

The ability to describe both extensional and steady shear behaviour with a common set of Giesekus fluid parameters was tested and shown to depend on whether the solution is in the dilute or entangled regime. Figure 2(*a*) shows that the Giesekus model, Equation [5], gives a good description of the linear shear rate data in the semi-dilute regime (5 g/L): previously we (Torres *et al.*, 2014b) reported the transition from the semi-dilute to an entangled regime for these aqueous guar gum solutions to lie around 5 g/L. Figure 2(*b*) shows that the fit at 10 g/L is less good, which is attributed to entanglement effects. The highest deviations were found above 350 s^{-1}, which lie in the range of those experienced at the wall of the planetary mixer.

Equation [5] has four adjustable parameters; the zero shear rate viscosity, the infinite shear rate viscosity, the Giesekus mobility parameter and the relaxation time. η_∞ was set at zero and the remaining parameters were fitted to the experimental data by a least squares algorithm. The results for 5 g/L solutions are listed in Table 2, with the fitted η_0 values close to those measured at the lowest shear rate studied, 0.01 s^{-1}. Two sets of parameters are reported: one obtained by fitting steady shear and extensional data (presented later), and a second set obtained by fitting the extensional data alone. The η_0 values were consistent with ones previously reported for unareated aqueous guar gum solutions with concentrations between 0.39-0.97 g/L (Bourbon *et al*. (2010)), and for unaerated hydroxypropyl ether guar gum solutions at concentrations up to 5 g/L (Duxenneuner *et al.*, 2008). These studies also found the relaxation time to increase with increasing polymer concentration, which is evident in comparing the values for 5 g/L (Table 2) and 10 g/L (Table 3) solutions. The relaxation time for the 5 g/L guar gum solution is comparable with the values given by Bourbon *et al*. (2010), wherein they modelled the solutions as a FENE material: they reported two relaxation times, with values from $\lambda_1 \sim 15$ ms and $\lambda_2 \sim 1$ ms for 1.9 g/L, and $\lambda_1 \sim 58$ ms and $\lambda_2 \sim$ 4200 ms for 9.7 g/L. It should be noted, however, that the FENE model did not give good agreement with their experimental data. They attributed the two relaxation times to arise from this the structure of the polysaccharides, one related to the expansion of the polymeric chains, the other relating to interactions between the chains delaying the relaxation phase.

The effect of air volume fraction on the relative viscosity at low shear rate, η_{r0}, for solutions prepared with and without syringing is presented in Figure 3. The relative viscosity was calculated by dividing the measured apparent viscosity by that measured for the centrifuged guar gum solution ($\phi = 0$) at the same shear rate, 0.1 s^{-1}. This shear rate corresponded to $Ca < 0.01$ for each case and under these conditions the bubbly liquid is expected to behave as a suspension. Both 5 g/L and 10 g/L guar gum solutions exhibit a linear dependency on ϕ, with the result for 5 g/L, $\eta_{r0} = 1 + 1.03\phi$ (regression coefficient, $R^2 = 0.993$) following the classical Taylor (1932) result $\eta_r = 1 + \phi$. The 10 g/L result, $\eta_{r0} = 1 + 1.25\phi$, fits the trend, $\eta_r = 1 + a\phi$, derived by Stein and Spera (1992) for dilute emulsions with no bubble deformation.

The steady shear results could also be fitted to the Cross model, Equation [A.1], with satisfactory agreement ($R^2 > 0.997$), as shown in the Appendix. The Cross model, however, does not provide insight into the extensional behaviour, discussed later, and this agreement is reported for completeness and for comparison with other studies of similar solutions.

Oscillatory shear measurements

Figure 4 shows selected mechanical spectra (G' and G'' vs. angular frequency) of centrifuged guar gum solutions and their bubbly liquids following 10 min aeration ($\phi = 0.25$). The frequency dependency of the centrifuged gum solutions follows the trend reported elsewhere for similar solutions (Steffe, 1996; Torres *et al.* 2013; Torres *et al.* 2013). Figure 4(*a*) shows that $G'' > G'$ for samples in the semi-dilute regime (5 g/L) over the frequency range studied, indicating predominantly viscous behaviour, whereas there is a crossover for those in the entanglement regime (10 g/L) and the elastic response prevails at higher frequencies (Figure 4(*b*)). The data sets show a strong frequency dependency, with both moduli increasing by three orders of magnitude between 0.1 and 10 Hz. These results are similar to those reported for several other random coil polymers (Brummer *et al.*, 2003; Sittikiyothin *et al.*, 2005; Bourbon *et al.*, 2010).

The mechanical spectra in Figure 4 show that aeration ($\phi \sim 0.25$) increases both the viscous and elastic nature of the liquids. For bubbly liquids prepared at 10 g/L, the crossover frequency (where

399 $G' \sim G''$) was found to be independent of ϕ, at 4 Hz, indicating that this feature is related to the
400 properties of the continuous phase. Similar trends were reported by Sahu and Niranjan (2009) for
401 whipped cream, who noted that even though the continuous phase may be purely viscous, bubble
402 incorporation tends to make the dispersion viscoelastic.
403
404 The values of G' and G'' for intermediate ϕ values lay between the data sets on Figure 4: the
405 enhancement in G' due to the bubble phase, expressed $G'(\phi)/G'(0)$, in analogy with work on
406 suspensions by (for example, Bossard, 2008), at frequencies of 0.1, 1.0 and 10 Hz is plotted in
407 Figure 5. A common, almost linear, enhancement is evident for the 5 g/L gum-based liquids for all
408 three frequencies. The results for the 10 g/L gum-based liquids in Figure 5(*b*) show almost linear
409 dependencies on ϕ, which decrease as the frequency approaches the crossover frequency of 4 Hz,
410 where there is no enhancement due to the bubble phase. Figure 5(*c*) presents the phase angle as a
411 function of air volume fraction at different angular frequencies. All the phase angle profiles are
412 frequency dependent. The data for 10 g/L-based liquids at 0.1 Hz show similar dependency on ϕ to
413 the 5 g/L liquids, but the phase angle decreases noticeably at higher frequencies for this entangled
414 solution. This can be explained qualitatively as the response at higher frequencies becoming
415 dominated by the characteristic time of the continuous phase.
416
417 No statistically significant effect of syringing on G' and G'' was observed for bubbly liquids with
418 similar ϕ values, even when the bubbles in the syringed samples were noticeably smaller than those
419 prepared without syringing. Noticeable differences were observed in our previous study (Torres *et*
420 *al.*, 2013), where the bubbly liquids were prepared with rheologically different liquid phases. In that
421 work, bubbly liquids were prepared with 10 g/L aqueous solutions of guar gum (as studied here) and
422 a viscous liquid, honey (almost constant shear viscosity, similar to η_0 for the guar gum, with a small
423 elastic contribution). The bubbles in the honey were noticeably smaller (mode around 40 μm) than
424 in the guar gum (mode around 80 μm). The bubbly liquids were prepared using the same protocols,
425 yielding similar ranges of ϕ, but the increase in G' and G'' on aeration was noticeably smaller for the
426 shear-thinning liquid.

The above results confirm that the rheology and processing of a bubbly liquid is intimately related to the nature of the continuous phase as well as the bubble volume fraction and bubble behaviour.

Extensional measurements

Figure 6 shows the evolution of mid-filament diameter, D_{mid}, for centrifuged guar gum solutions and the bubbly liquids prepared with different air volume fractions. The solid lines show the data obtained with syringed samples. The diameter is determined by the balance of surface tension and viscous/elastic forces: viscous forces tend to stabilize the filament, while surface tension acts to destabilize it, causing the increasingly rapid decrease in the diameter until the filament breaks apart. The decrease in D_{mid} with time is not linear: there is a sharp step to point A followed by an exponential decay, after which the rate of decay increases towards break-up at time t_F. Similar trends were reported for other aqueous guar gum systems in the absence of bubbles (Duxenneuner *et al*., 2008; Bourbon *et al*., 2010; Torres et al., 2014a), and confirms non-Newtonian behaviour.

Samples prepared with syringing gave smoother profiles, and a tended to exhibit a slightly smaller t_F value. Noticeable differences are evident in the profiles for the 10 g/L liquids with ϕ>0.20: the whisked materials feature oscillations that disappear when D_{mid} approaches the modal bubble diameter in Figure 1(*c*). Thereafter the profiles for samples prepared with and without syringing tend to a common t_F value. The oscillations could be attributable to the hindered motion of the bubbles with respect to one another at high volume fraction within a liquid of relatively high viscosity (compared to 5 g/L). The absence of an oscillatory trend in the data derived from tests at 5 g/L, at a comparable bubble volume fraction, suggests that the viscosity of the continuous phase, in addition to the bubble volume fraction, is important in determining the dynamics of the liquid thread. Additional investigation is required to elucidate the mechanism involved.

The time to break-up increased linearly with ϕ for both guar gum solutions. Linear regression of the aerated data (Figure 7(a)) gave:

$$\text{(5 g/L)} \quad t_F = 443\phi + 62.8 \qquad R^2=0.991 \qquad (13)$$

(10 g/L) $t_F = 564\phi + 83.2$ R^2=0.985 (14)

The intercepts in both the above relationships lie below the values obtained for the centrifuged solutions. Further work with small air fractions ($0 < \phi < 0.05$) is required to establish the onset of bubble influence. The t_F values also increased with D_1 (Figure 7(*b*)), following exponential dependencies:

(5 g/L) $t_F = 2.42\exp(0.008D_1)$ R^2=0.990 (15)

(10 g/L) $t_F = 0.78\exp(0.010D_1)$ R^2=0.999 (16)

A similar dependency between t_F and D_1 was reported for cake batters by Chesterton *et al.* (2011a). In that case the liquid phase was a shear-thinning suspension of flour particles in an aqueous emulsion.

Figure 8 presents the data in Figure 6 in the alternative form reported by Chesterton *et al.* (2011), where the capillary diameter, normalised as in Equation [17], is plotted against time normalised against t_F. The data sets collapse to a common form with the exception of those prepared with 10 g/L guar gum solution (entanglement regime) and $\phi > 0.20$ without syringing. After the initial transient, the data for $t/t_F < 0.6$ follow the form

$$\frac{D_{mid}(t)}{D_1} \propto \exp\left(-\frac{t}{t_F}\right) \quad (17)$$

Chesterton *et al.* (2011) reported similarly good data reduction for cake batters prepared using several different flours while Torres *et al.* (2014a) demonstrated the same result for aqueous guar gum solutions with concentrations ranging from 1-20 g/L. Plotting the filament stretching data in terms of the capillary time (Equation [12]) gave no useful insight other than confirming that these bubbly liquids did not exhibit the behaviour reported by Anna and McKinley (2001).

Torres *et al.* (2014b) showed that Equation [11] is able to reproduce this behaviour and its suitability for these bubbly liquids is demonstrated by Figure 9 where the non-dimensional filament diameter is plotted against absolute time for (*a*) the semi-dilute guar gum solutions (5 g/L) and for the entangled guar gum solutions (10 g/L) (*b*) without and (*c*) with syringing.

Figure 9(*a*) shows the data obtained with the 5 g/L guar gum solutions, where there was no statistically significant effect of syringing. Two sets of loci are plotted on this Figure: the solid loci show the behaviour predicted for a single mode Giesekus fluid, *i.e.* Equation [11], with the parameters obtained from regression of both the steady shear (Figure 2) and extension (this plot), listed in Table 2. The surface tension was taken from Torres *et al.* (2014a). The dotted loci are obtained by fitting Equation [11] to the extensional data alone, and the parameters obtained are presented alongside those above in Table 2. In both cases, Equation [11] gives a good description of the initial decay in filament diameter, and an excellent description of the approach to t_F: the fit to the data in the region $D/D_1 = 0.2 \rightarrow 0.05$ is less successful. The R^2 values for the fitting to both linear and extensional shear are, in each case, not as good as fitting the extensional shear alone, but the difference is small (at worst, 0.979 *cf.* 0.990 for $\phi = 0.25$) and is considered acceptable here in applying the model across two very different deformation modes.

Figure 9(a) is significant as it indicates that a reasonable estimate of the extensional behaviour of the bubbly liquids, prepared using non-Newtonian solutions (here, a polymer solution in the semi-dilute regime), could be obtained by treating the system as a Giesekus fluid. The unaerated guar sum solutions exhibit Giesekus fluid behaviour and these results indicate that the presence of the bubble phase can be represented by modifying the Giesekus pararameters, in the same way that Llewellin *et al*. (2002) reported that a modified Jeffreys fluid model could be used to describe bubbly liquids prepared with a Newtonian liquid phase.

At concentrations of 10 g/L, where entanglement is apparent, and where there is an associated increase in the magnitude of the elastic response (Torres et al., 2013), Equation [11] does not give a good prediction of the extensional behaviour when the parameters obtained from linear shear data, Equation [5], are used (data not shown). Figures 9(*b*) and (*c*) show that Equation [11] gives a reasonable fit to the data from the 10 g/L solutions if the mobility parameter and relaxation time are fitted solely to these extensional data; similar results have been reported in Torres *et al.* (2014b). The model is understandably unable to give a good description of the data sets with oscillations (*i.e.* $\phi >$

512 0.20 without syringing). The values of D_1, η_0, η_∞, α, a and λ are reported alongside those obtained
513 from linear shear in Table 3.
514
515 The influence of ϕ on the Giesekus model parameters in Tables 2 and 3 is now reviewed. Figure 3
516 shows a linear dependency of $\eta_{r,o}$ on ϕ for both solutions, and Figure 10 summarises the effect of ϕ
517 on the relaxation time and mobility parameter. Two sets of parameters are presented for the semi-
518 dilute (5 g/L) liquid phase; those obtained from fitting both modes and those obtained solely from
519 extensional data. For the former, λ increases modestly with ϕ and a decreases with ϕ, both
520 exhibiting a linear trend on these log-linear plots. When extensional data alone are fitted separately
521 (solid squares), λ increases exponentially with ϕ (approaching the λ value for linear shear at $\phi = 0.25$)
522 and a is almost constant, at ~0.03 (*cf* ~ 0.05 for steady shear fitting). These results indicate that the
523 curve fitting problem is poorly posed, in that there are likely to be several optima. The steady shear
524 behaviour predicted using the extensional shear parameters in Table 2 did not agree well with the
525 results in Figure 2 (data not reported), indicating that estimating steady shear results from
526 extensional measurements of this quality is not reliable.
527
528 In the entanglement regime (10 g/L), Table 3 and Figure 10(*b*) shows that a is almost constant as
529 ϕ increases from 0 to 0.25. In contrast, Figure 10(*a*) shows that while λ is relatively insensitive to ϕ
530 for linear shear (as observed with 5 g/L liquids), it increases strongly with ϕ for the extensional data
531 fitting. Similar values (and trends) were seen for both whisked and syringed samples: the parameters
532 only differ noticeably at higher ϕ values, which is attributed to the oscillations evident in the
533 whished samples.
534
535 Duxenneuner *et al*. (2008) studied modified guar gum solutions and reported that the relaxation time
536 followed a power-law scaling dependency in the semi-dilute concentration regime ($3c^*$ up to $9c^*$,
537 with c^* being the critical concentration ~ 0.58 g/L). They stated that this was due to increasing
538 interactions between hydroxypropyl ether gum molecules in solution with increasing concentration.
539 This behaviour was only noticed in the present work for aqueous guar gum solutions prepared in the

entanglement regime; previous work (Torres *et al.*, 2014b) has reported the onset of the entanglement regime at concentrations between 5 g/L and 10 g/L.

Figure 11(*a*) shows the relationship between the two timescales describing the filament extension, namely the break-up time observed in experiments, t_F, and the relaxation time estimated from the Giesekus model. All three data sets exhibit an increasing trend. For the 5 g/L data sets, the Figure confirms that quite different λ values are obtained when this parameter is fitted solely to extensional data rather than being constrained such that it additionally fits the linear shear data. The unconstrained 5 g/L and 10 g/L values, fitted to extensional data alone, follow a similar trend (although a differs noticeably), with the 10 g/L data approaching an asymptote of $t_F \sim 225$ ms. This difference in parameters arising from the choice of constraint when fitting the data indicates that the parameters a and λ are correlated and further information, preferably linked to independent measurements, is required for definitive estimates.

The extent of correlation in these Giesekus parameters can be gauged by examining the limiting behaviour of Equation [11]. As the non-dimensional filament diameter tends to zero, the time, t, tends to the filament rupture time, t_F. As $D/D_1 \rightarrow 0$, Equation [11] gives

$$(4a-3)\ln\left(\frac{2aA}{1+2aA}\right)+\frac{2}{A}=\frac{t_F}{\lambda} \tag{18}$$

where

$$A=\frac{\lambda\alpha}{\eta_0 D_1} \tag{19}$$

t_F can then be estimated from Equation [18] for the parameter sets in Figure 11(*a*), and in Tables 2 and 3. Figure 11(*b*) shows excellent agreement between the estimated t_F values and those obtained experimentally. This result highlights that the form of Equation [11] forces the regression to fit the measurements around the break-up time.

Extensional viscosity

The apparent extensional viscosity was estimated using Equation [9]. This analysis assumes that the equilibrium surface tension values can be used to estimate the forces involved in extension; direct measurement of the force in the filament is required to confirm these values. Figure 12 displays the apparent extensional viscosity as a function of the Hencky strain of centrifuged guar gum solutions prepared at (*a*) 5 g/L and (*b*) 10 g/L and the corresponding bubbly liquids obtained after 10 min aeration as representative examples. Data sets obtained at lower ϕ exhibited similar trends. Since the apparent extensional viscosity profiles are a function of the mid-filament diameter, D_{mid}, which itself changes as a function of time, the values are governed by the self-thinning of the filament, and are not a response to an imposed shear rate as in shear rheometry. The extensional viscosities increase sharply at low Hencky strains, exhibiting a peak (at $\varepsilon \sim 1.2$) for centrifuged solutions at 10 g/L, where entanglement is believed to be important. At higher strains, η_e approaches an asymptote. In the case of the bubbly liquids, η_e at a given Hencky strain increases with air volume fraction, which is consistent with the observed increase in η_{app} with air volume fraction. Qualitatively, the trend of η_e as a function of ε is the same for both aerated and de-aerated liquids. Similar trends and parameter values were found for the bubbly liquid samples after syringing.

According to Liang and Zhong (2013), the extensional viscosity for polymeric fluids which exhibit Cross model behaviour can be estimated using:

$$\eta_e = \frac{3\eta_0}{1 + k\dot{\varepsilon}^{(1-n)}} \tag{20}$$

where *k* is the Cross model time constant and *n* is the follow index. In their approach, the shear rate is replaced by Hencky strain rate, $\dot{\varepsilon}$. The extensional viscosities predicted for unaerated and strongly aerated (ϕ = 0.25) bubbly liquids in Figure 12 do not follow the trend calculated from the filament stretching tests, and highlight the need to study extensional behaviour of these materials.

Conclusions

The shear and extensional rheology of bubbly liquids based on two guar gum solutions, with bubble volume fractions between 0.00 and 0.25, was studied. The behaviour of the un-aerated solutions was viscoelastic, as reported previously (Torres et al., 2014a), with the 5 g/L solution being in the semi-dilute regime and the 10 g/L in the entanglement regime (Torres et al., 2014b). Preparing the samples by whisking followed by syringing modified the bubble sizes from a log-normal distribution with a mode of 80 μm to one with a mode of 30 μm.

The steady shear data revealed that shear response of the fluid was largely independent of the bubble size. Increasing the bubble volume fraction, however, increased the elastic and viscous moduli of the liquids noticeably, in addition to changing the dominant behaviour mode; for example, the crossover between elastic and viscous dominance occurred at a lower frequency for a 10 g/L solution with bubble volume fraction of 0.25 compared to an un-aerated solution.

The filament stretching data highlighted that the dynamics of the filament thinning were affected by the bubble size distribution, but that the filament rupture time was largely independent of this factor. The filament rupture time was dependent on both the solution concentration and the bubble volume fraction; increasing both of these parameters resulted in longer rupture times, with a linear relationship evident between the rupture time and the bubble volume fraction. Time-concentration superposition of the filament stretching data gave a single mastercurve for 5 g/L data for all bubble volume fractions and for 10 g/L data with bubble volume fractions less than 0.20. This time-concentration superposition has been reported in previous work on food fluids (Chesterton et al., 2011a; Torres et al., 2014a).

A single mode Giesekus fluid could be used to model the rheological properties of the fluids in both shear and extension. For guar gum concentrations of 5 g/L, it was found that a common mobility parameter and relaxation time could describe both the shear and extensional behaviour of the fluids. In the entanglement regime, at guar gum concentrations of 10 g/L, it was not possible to fit both the shear and extensional characteristics of the solutions using a common set of Giesekus parameters;

620 this could be remedied by extending the theory to make using a multi-mode Giesekus approach and
621 will be the subject of a future study.
622
623 It was possible, however, to obtain Giesekus parameters uniquely for shear or extension. These
624 results are consistent with previous work in this area (Torres et al., 2014b). In all cases, the Gieskus
625 parameters exhibited monotonic dependency on bubble volume fraction, which can be used to
626 interpolate for intermediate values. Further experimental and theoretical work is required to establish
627 whether these trends can be applied to other bubbly liquids based on a Giesekus fluid continuous
628 phase.
629

630 **Acknowledgements**
631 The authors acknowledge the financial support (POS-A/2012/116) from Xunta de Galicia's
632 Consellería de Cultura, Educación e Ordenación Universitaria of Spain and the European Union's
633 European Social Fund.

References

Abivin P., Henaut I., Argillier J-F., Moan M. (2009) Rheological behavior of foamy oils, Energy & Fuels, 23, 1316–1322.

Ahmed R.M., Takach N.E., Khan U.M., Taoutaou S., James S., Saasen A., Godøy R. (2009) Rheology of foamed cement, Cement and Concrete Research, 39, 353–361.

Allais, I., Edoura-Gaena, R.B., Gros, J. B., & Trystram, G. (2006). Influence of egg type, pressure and mode of incorporation on density and bubble distribution of a lady finger batter. *Journal of Food Engineering*, 74, 198-210.

Anna, S.L., & McKinley, G.H. (2001). Elasto-capillary thinning and breakup of model elastic liquids. *Journal of Rheology*, *45*, 115-138.

Bird, R.P., Curtiss, C.F., Armstrong, R.C., & Hassager, O. (1987). *Dynamics of Polymeric Liquids*. (2nd ed.). New York: Wiley-Interscience, (Volumen 2: Kinetic Theory).

Brummer, Y., Cui, W., & Wang, Q. (2003). Extraction, purification and physicochemical characterization of fenugreek gum. *Food Hydrocolloids*, 17, 229-236.

Bossard, F. (2008). Linear and nonlinear viscoelastic behavior of very concentrated plate-like kaolin suspensions. *Journal of Rheology*, 51, 1253-1270.

Bourbon, A.I., Pinheiro, A.C., Ribeiro, C., Miranda, C., Maia, J.M., Teixeira, J.A., & Vicente, A.A. (2010). Characterization of galactomannans extracted from seeds of *Gleditsia triacanthos* and *Sophora japonica* through shear and extensional rheology: Comparison with guar gum and locust bean gum. *Food Hydrocolloids, 24*, 184-192.

Chenlo, F., Moreira, R., & Silva, C. (2010). Rheological properties of aqueous dispersions of tragacanth and guar gums at different concentrations. *Journal of Texture Studies, 41*, 396-415.

Chesterton, A.K.S., Pereira de Abreu, D.A., Moggridge, G.D., Sadd, P.A., Wilson, D.I. (2013). Evolution of cake batter bubble structure and rheology during planetary mixing, *Food and Bioproducts Processing*, 91, 192-206.

Chesterton, A.K.S., Meza, B.E., Moggridge, G.D., Sadd, P.A., & Wilson, D.I. (2011a). Rheological characterisation of cake batters generated by planetary mixing: elastic versus viscous effects. *Journal of Food Engineering, 105*, 332-342.

Chesterton, A.K.S., Moggridge, G. D., Sadd, P.A., Wilson, D.I. (2011b). Modelling of shear rate distribution in two planetary mixtures for studying development of cake batter structure. Journal of Food Engineering, 105, 343-350.

Cross, M.M. (1965). Rheology of non-Newtonian fluids: a new flow equation for pseudoplastic systems. *Journal of Colloid Science, 20*, 417-437.

Duxenneuner, M.R., Fischer, P., Windhab, E.J., & Cooper-White, J.J. (2008). Extensional properties of hydroxypropyl ether guar gum solutions. *Biomacromolecules, 9*, 2989-2996.

Eggers, J. (1997). Nonlinear dynamics and breakup of free-surface flows. *Reviews of Modern Physics*, 69(3), 865-926.

671 Gabriele D., Baldino N., Migliori M., de Cindio B., Tricarico C. (2012) Modelling flow behaviour of
672 dairy foams through a nozzle. Journal of Food Engineering, 109, 218-229.
673 Giesekus, H. (1982). A simple constitutive equation for polymer fluids based on the concept of
674 deformation-dependent tensorial mobility. *Journal of Non-Newtonian Fluid Mechanical, 11*,
675 69-109.
676 Golemanov K., Tcholakova S., Denkov N.D., Ananthapadmanabhan K.P., Lips A. (2008) Breakup
677 of bubbles and drops in steadily sheared foams and concentrated emulsions. Physical Review
678 E, 78, 051405-1-051405-12.
679 Gonnermann, H.M., & Manga, M. (2007). The fluid mechanics inside a volcano. *Annual Review of*
680 *Fluid Mechanics*, 39,321-356
681 Grace, H.P. (1982). Dispersion phenomena in high viscosity immiscible Fluid systems and
682 application of static mixers as Dispersion devices in such systems. *Chemical Engineering*
683 *Communications*, 14, 225-277.
684 Gupta, R.K., Nguyen, D.A., & Sridhar, T. (2000). Extensional viscosity of dilute polystyrene
685 solutions: Effect of concentration and molecular weight. *Physics of Fluids, 12*, 1296-1318.
686 Jakubczyk E. & Naranjan K. (2006). Transient development of whipped cream properties. *Journal of*
687 *Food Engineering*, 77.1, 79-83.
688 Larson, G. (1988). *Constitutive Equations for Polymer Melts and Solutions.* Boston: Butterworths.
689 Liang, J.-Z., Zhong, L. (2013). Characterization of elongation viscosity for polyethylene melts.
690 *Colloid and Polymers Science*, 291, 1595-1599.
691 Llewellin E.W., Mader H.M., Wilson S.D.R. (2002) The rheology of a bubbly liquid. Proceedings of
692 the Royal Society of London Series A-Mathematical Physical and Engineering Sciences, 458,
693 987-1016.
694 Malysa K., Lunkenheimer K. (2008) Foams under dynamic conditions. Current Opinion in Colloid
695 and Interface Science, 13, 150-62.
696 Manga M., Loewenberg M. (2001) Viscosity of magmas containing highly deformable bubbles.
697 Journal of Volcanology and Geothermal Research, 105**,** 19-24.
698 McKinley, G.H., & Tripathi, A. (2000). How to extract the Newtonian viscosity from capillary
699 breakup measurements in a filament rheometer. *Journal of Rheology, 44*, 653-670.
700 Meza, B.E., Chesterton, A.K.S., Verdini, R.A., Rubiolo, A.C., Sadd, P.A., Moggridge, G.D., &
701 Wilson, D.I. (2011). Rheological characterisation of cake batters generated by planetary
702 mixing: Comparison between untreated and heat-treated wheat flours. Journal of Food
703 Engineering, *104*, 592-602.
704 Rust A.C., Manga M. (2002) Effects of bubble deformation on the viscosity of dilute suspensions.
705 Journal of Non-Newtonian Fluid Mechanics, 104, 53-63.
706 Sahu, J.K., & Niranjan, K. (2009). Gas–liquid mixing. In: Cullen, P.J. (Ed.), Food Mixing:
707 Principles and Applications. Wiley-Blackwell.

Schleiniger, G., 1991. A remark on the Giesekus viscoelastic fluid. *Journal of Rheology*, 35, 1157.

Steffe, J.F. (1996). *Rheological Methods in Food Process Engineering*, Michigan: Freeman Press.

Stein, D.J. & Spera, F.J. (1992). Rheology and microstructure of magmatic emulsions: theory and experiments. *Journal of Volcanology and Geothermal Research*, 49**,** 157-174.

Sittikijyothin, W., Torres, D., & Gon**ç**alves, M.P. (2005). Modelling the rheological behaviour of galactomannan aqueous solutions. *Carbohydrate Polymers*, 59, 339-350.

Taylor, G.I. (1932). The viscosity of a fluid containing small drops of another fluid. *Proceedings of the Royal Society of London, Series A*, 138, 41-48.

Thakur R.K., Vial C.H., Djelveh G. (2003) Influence of operating conditions and impeller design on the continuous manufacturing of food foams. *Journal of Food Engineering*, 60, 9-20.

Thompson M.J., Pearson J.R.A., Mackley M.R. (2001) The effect of droplet extension on the rheology of emulsions of water in alkyd resin. *Journal of Rheology*, 45, 1341-1358.

Tatham, J.P., Carrington, S., Odell, J.A., Gamboa, A.C., Muller, A.J., & Saez, A.E. (1995). Extensional behavior of hydroxypropyl guar solutions: Optical rheometry in opposed jets and flow through porous media. *Journal of Rheology*, *39*, 961-986.

Torres, M.D., Gandala-Maria, F., & Wilson, D.I. (2013). Comparison of the rheology of bubbly liquids prepared by whisking air into a viscous liquid (honey) and a shear-thinning liquid (guar gum solutions). *Journal of Food Engineering*, *118*, 213-228.

Torres, M.D., Hallmark, B., Wilson, D.I. (2014a). Effect of concentration on shear and extensional rheology of guar gum solutions. *Food Hydrocolloids*, 40, 85-95.

Torres, M.D., Hallmark, B., Hilliou, L., Wilson, D.I. (2014b). The single mode Giesekus equation as a model for describing the shear and extensional behaviour of complex food fluids. *AIChEJ*, in press.

van Aken G.A. (2001). Aeration of emulsions by whipping. *Colloids Surface A, 190*, 333-354.

Vadillo, D.C., Mathues, W., & Clasen, C. (2012). Microsecond relaxation processes in shear and extensional flows of weakly elastic polymer solutions. *Rheologica Acta*, *51*, 755-769.

Vadillo, D.C., Tuladhar, T.R., Mulji, A.C., Jung, S., Hoath, S.D., & Mackley, M.R. (2010). Evaluation of the inkjet fluid's performance using the ''Cambridge Trimaster'' filament stretch and break-up device. *Journal of Rheology*, *54*, 261-282.

Yoo, J.Y., Choi, H.C., 1989. On the steady simple shear flows of the one-mode Giesekus fluid. *Rheologica Acta*, 28, 13-24.

A. Appendix: Cross model

The shear-thinning behaviour of bubbly liquids prepared using aqueous guar gum solutions was fitted to the Cross-Williamson model (Cross, 1965) and representative examples are given in Figure A.1:

$$\frac{\eta_{app}}{\eta_0} = \frac{1}{1 + k\,\dot{\gamma}^{(1-n)}} \qquad \text{(A.1)}$$

where η_0 is the zero-shear rate viscosity, k is the time constant and n is the flow index.

(*a*) (*b*)

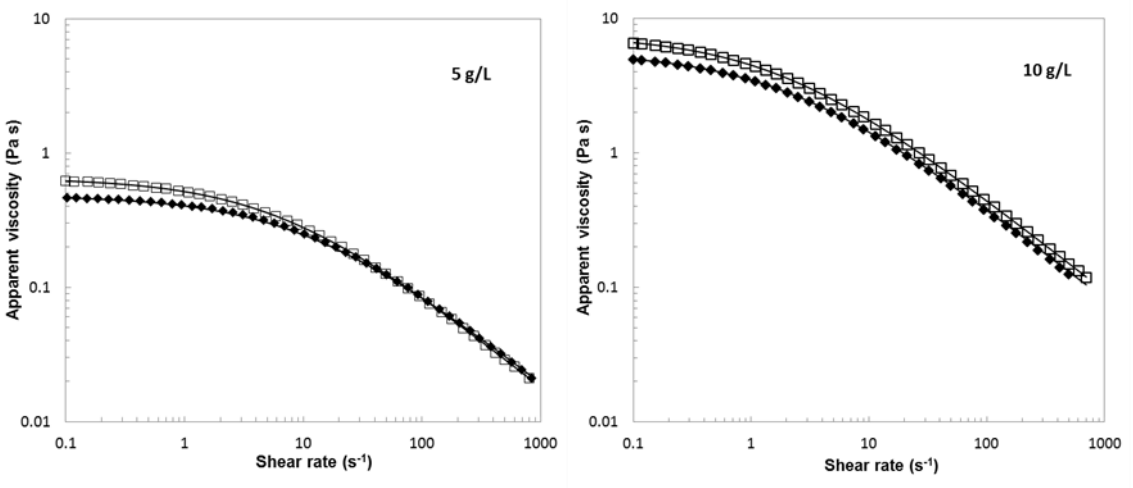

Figure A.1. Flow curves of representative aqueous guar gum solutions prepared at (a) 5 g/L and (b) 10 g/L. Symbols: diamonds – $\phi \approx 0$, squares – $\phi \approx 0.25$. Solid lines show the best fit obtained with the Cross model (Equation [A.1]).

The experimental data for guar gum samples were satisfactorily fitted ($R^2 > 0.997$) to the Cross-Williamson model, Equation [A.1], and the parameters η_0, k and n obtained are summarised in Table A.1. The η_0 value are those reported for the Giesekus model fitting in Tables 2 and 3 . The variation in k and n was modest, achieving similar values to those reported for synthetic polymer solutions. These results were consistent with previous studies of other guar gum solutions (Bourbon *et al.*, 2010; Duxenneuer *et al.*, 2008).

Figure Captions

Figure 1 Bubbly liquids ($\phi \approx 0.25$) prepared with (*a*) 5 g/L and (*b*) 10 g/L guar gum solutions. Bubble number size distributions in (*c*) show log-normal fits based on the radii for 5 g/L (dashed lines) and 10 g/L (solid lines) guar gum. Grey lines show trends obtained after syringing.

Figure 2 Flow curves of representative aqueous guar gum solutions prepared at (*a*) 5 g/L and (*b*) 10 g/L. Symbols: diamonds – $\phi \approx 0$, squares – $\phi \approx 0.25$. Dashed lines show Giesekus model (Equation [5]) with parameters in Table 2. In this and subsequent plots, error bars are not plotted if the uncertainty in data values is smaller than the symbol size. The same scale is used on the ordinate axes here and is later plots to facilitate comparison between concentrations.

Figure 3 Effect of air volume fraction on guar gum bubbly liquid low shear rate relative viscosity at 0.1 s^{-1}: (*a*) 5 g/L and (*b*) 10 g/L. Dashed lines show linear trend obtained by regression, with $\eta_r = 1 + \phi$ ($R^2 = 0.993$) for 5 g/L and $\eta_r = 1 + 1.25\phi$ ($R^2 = 0.990$) for 10 g/L. Solid line on (*b*) shows the Taylor (1932) result, $\eta_{r0} = 1 + \phi$.

Figure 4 Mechanical spectra of representative aqueous guar gum solutions prepared at concentrations of (*a*) 5 and (*b*) 10 g/L. Symbols: closed – *G*', open – *G*", diamonds – $\phi \approx 0.00$, squares – $\phi \approx 0.25$

Figure 5 Effect of bubble volume fraction on elastic modulus for bubbly liquids prepared with (*a*) 5 g/L and (*b*) 10 g/L aqueous guar gum solution; (c) phase angle at selected frequencies. Symbols: squares – 5g/L, diamonds – 10 g/L, open – 0.1 Hz, grey – 1 Hz, black – 4 Hz. Dashed line in (*a*) shows fitted linear trend with $G'(\phi)/G'(0) = 1 + 4.3\phi$. Dashed line in (*b*) shows $G'(\phi)/G'(0)$ for bubbly liquids prepared at 5 g/L.

Figure 6 Effect of air volume fraction on evolution of dimensionless filament diameter for aqueous guar gum solutions prepared at (*a*) 5 g/L and (*b*) 10 g/L. Symbols: solid diamonds - $\phi \approx 0.00$, open diamonds – $\phi \approx 0.05$, circles - $\phi \approx 0.10$, triangles – $\phi \approx 0.15$, crosses – $\phi \approx$

0.20, squares – $\phi \approx 0.25$. Solid lines show experimental data obtained after syringing of the samples. The non-linear profiles indicate non-Newtonian behaviour.

Figure 7 Influence of (*a*) air volume fraction, ϕ, and (*b*) initial filament diameter (D_1) on filament break-up time (t_F). Symbols: diamonds – 10 g/L, squares – 5 g/L. Open symbols show trends obtained after syringing of the samples. Dashed lines show fitted trend lines, Eqns. [13, 14], solid trend lines show Eqns. [15, 16].

Figure 8 Dimensionless filament diameter - dimensionless time profiles for aqueous guar gum solutions prepared at (*a*) 5 g/L and (*b*) 10 g/L. Symbols: solid diamonds - $\phi \approx 0.00$, diamonds – $\phi \approx 0.05$, circles - $\phi \approx 0.10$, triangles – $\phi \approx 0.15$, crosses – $\phi \approx 0.20$, squares – $\phi \approx 0.25$.

Figure 9 Comparison of measured non-dimensional filament diameter with Giesekus model, Equation [11] for selected aqueous guar gum solutions prepared at (*a*) 5 g/L, (*b*) 10 g/L and (*c*) 10 g/L after syringing. Symbols: solid diamonds - $\phi \approx 0.00$, diamonds – $\phi \approx 0.05$, circles - $\phi \approx 0.10$, triangles – $\phi \approx 0.15$, crosses – $\phi \approx 0.20$, squares – $\phi \approx 0.25$. Solid loci in (*a*) show Equation [11] where parameters a and λ are those obtained from fitting both linear shear and extensional data, Table 2. Dashed loci show Equation [11] with parameters obtained by fitting to extensional data alone (Table 2 and Table 3).

Figure 10 Effect of air volume fraction on Giesekus model parameters: (*a*) relaxation time, λ, and (*b*) mobility parameter, a. Symbols: squares – 5 g/L, diamonds – 10 g/L. Open symbols, dashed lines – fitted to linear shear alone; solid symbols, solid lines – fitted to extensional data alone.

Figure 11 Correlation between (*a*) measured filament break-up time (t_F) and estimated relaxation time for guar gum bubbly liquids at different air volume fractions. (*b*) Comparison between experimental and predicted break-up times. Symbols: squares – 5 g/L, diamonds – 10 g/L. Open symbols denote 5 g/L data sets where the Giesekus parameters were obtained from steady shear measurements.

Figure 12 Effect of Hencky strain on apparent extensional viscosity of bubbly liquids generated by 10 min aeration ($\phi \approx 0.25$) of guar gum solutions at (*a*) 5 g/L and *(b*) 10 g/L. Solid symbols – $\phi \approx 0.00$, open symbols – $\phi \approx 0.25$. Dashed lines show the prediction for extension of a Cross model fluid estimated using Equation [20].

(*i*) after whisking (*ii*) after syringing

(*a*)

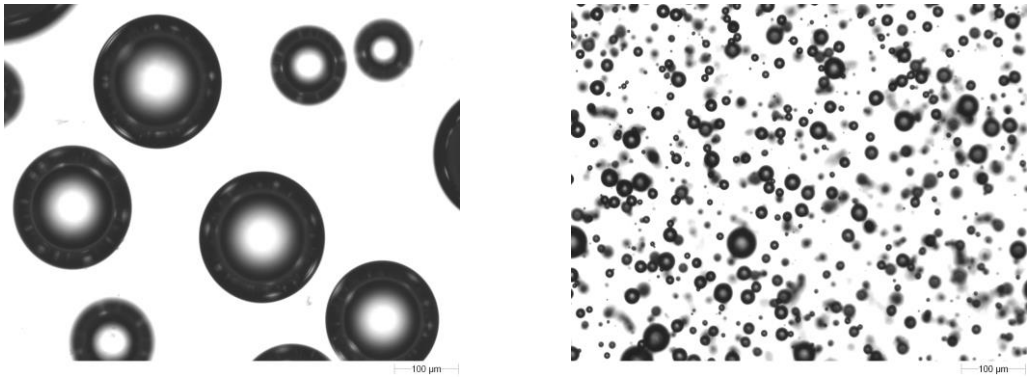

(*b*)

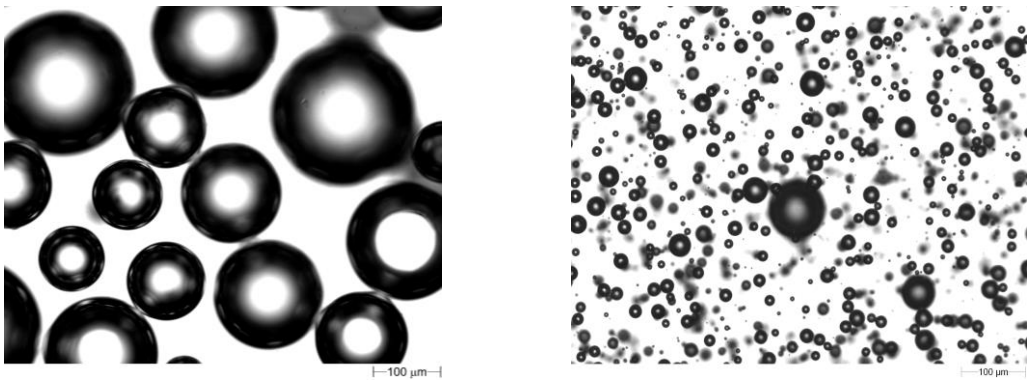

(*c*)

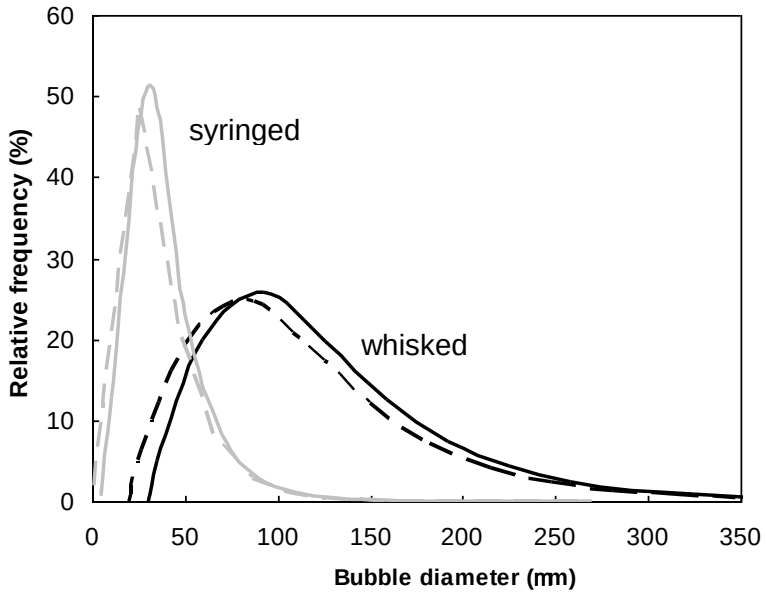

Figure 1 Bubbly liquids ($\phi \approx 0.25$) prepared with (*a*) 5 g/L and (*b*) 10 g/L guar gum solutions. Bubble number size distributions in (*c*) show log-normal fits based on the radii for 5 g/L (dashed lines) and 10 g/L (solid lines) guar gum. Grey lines show trends obtained after syringing.

(*a*)

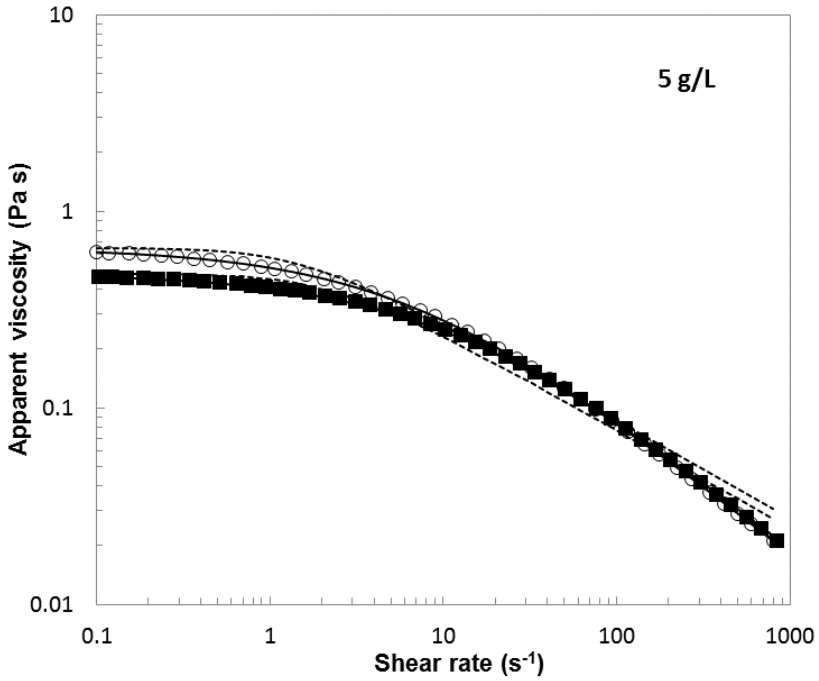

(*b*)

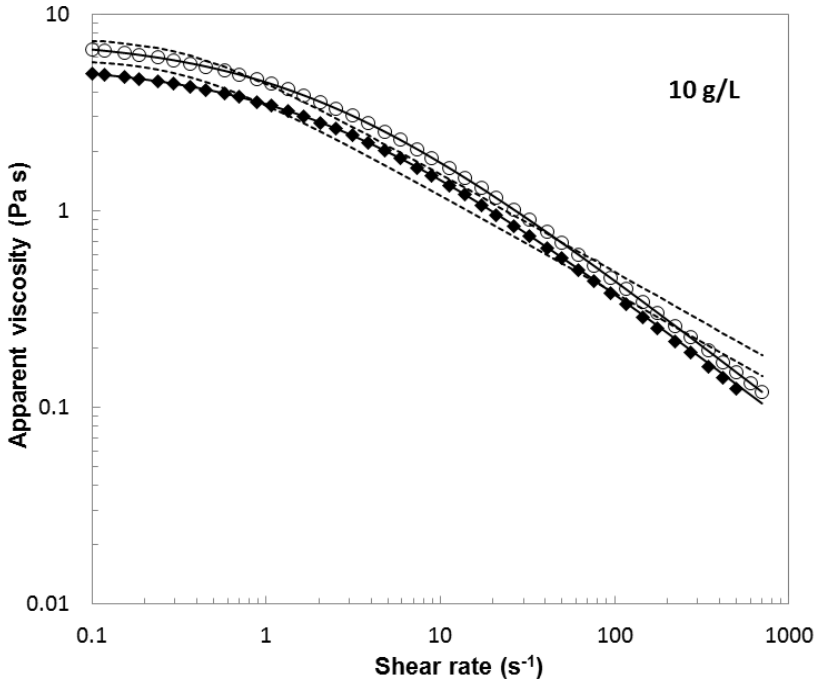

Figure 2 Flow curves of representative aqueous guar gum solutions prepared at (*a*) 5 g/L and (*b*) 10 g/L. Symbols: diamonds – $\phi \approx 0$, squares – $\phi \approx 0.25$. Dashed lines show Giesekus model (Equation [5]) with parameters in Table 2. In this and subsequent plots, error bars are not plotted if the uncertainty in data values is smaller than the symbol size. The same scale is used on the ordinate axes here and is later plots to facilitate comparison between concentrations.

(*a*)

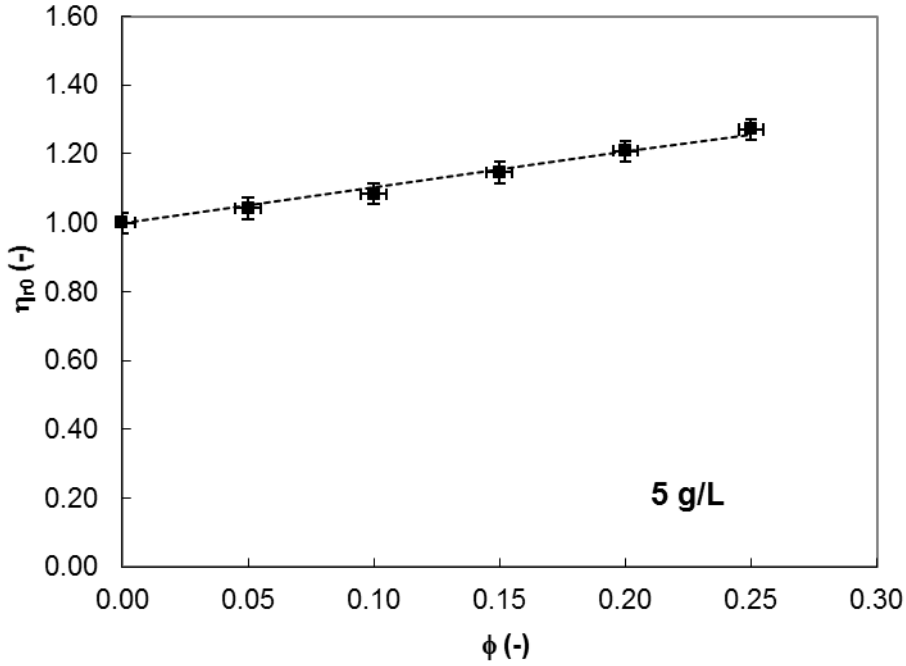

(*b*)

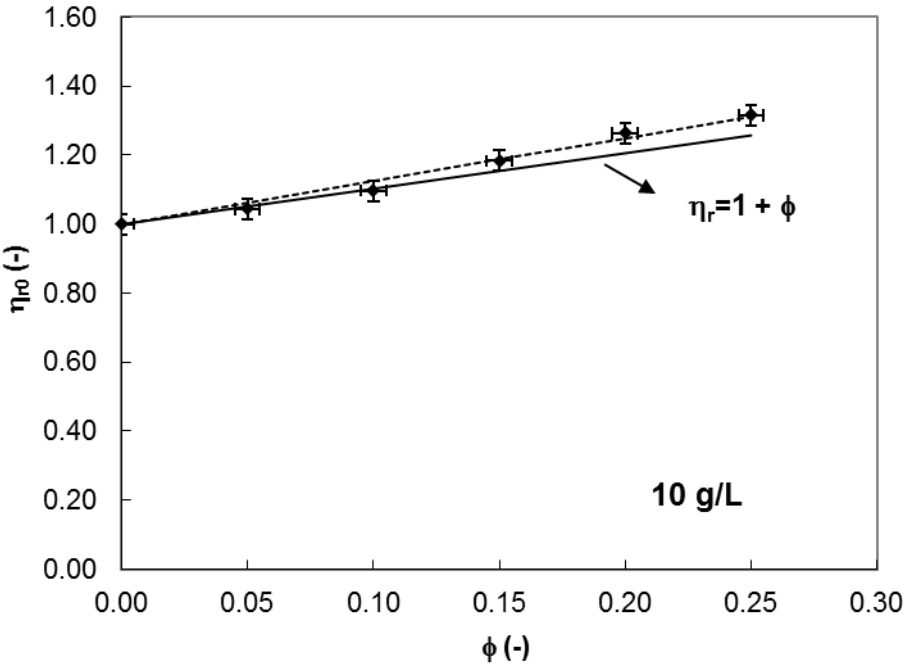

Figure 3 Effect of air volume fraction on guar gum bubbly liquid low shear rate relative viscosity at 0.1 s^{-1}: (*a*) 5 g/L and (*b*) 10 g/L. Dashed lines show linear trend obtained by regression, with $\eta_r = 1 + \phi$ ($R^2 = 0.993$) for 5 g/L and $\eta_r = 1 + 1.25\phi$ ($R^2 = 0.990$) for 10 g/L. Solid line on (*b*) shows the Taylor (1932) result, $\eta_{r0} = 1 + \phi$.

(*a*)

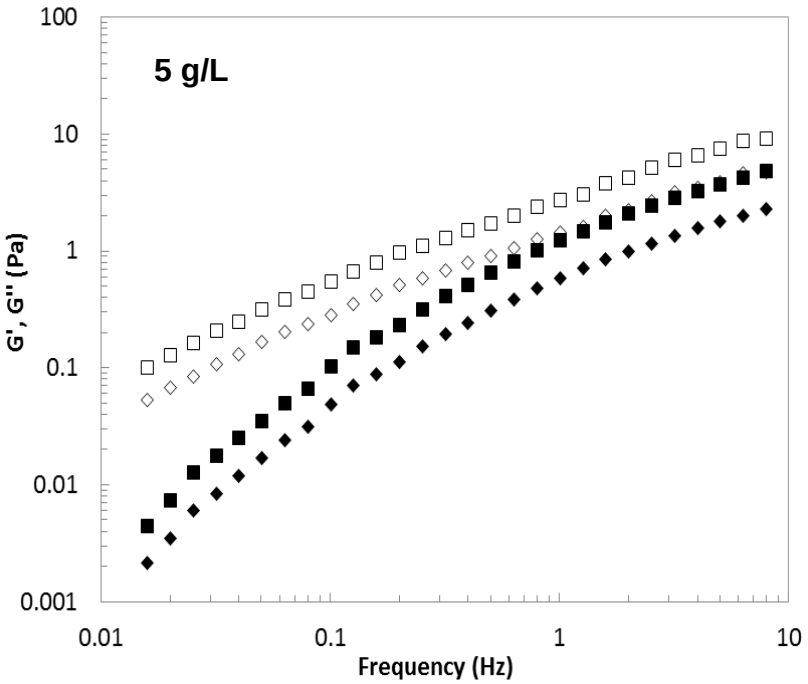

(*b*)

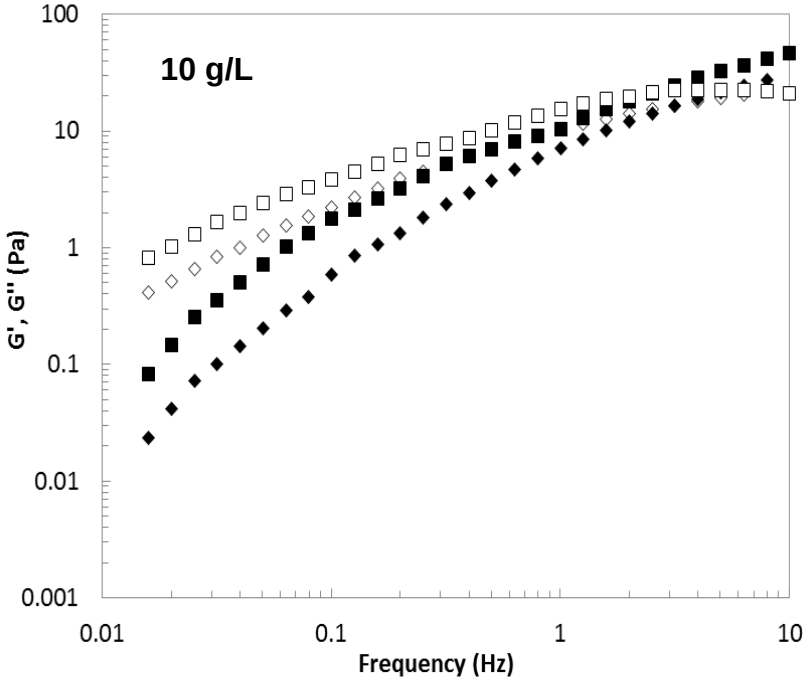

Figure 4 Mechanical spectra of representative aqueous guar gum solutions prepared at concentrations of (*a*) 5 and (*b*) 10 g/L. Symbols: closed – *G*', open – *G*", diamonds – $\phi \approx$ 0.00, squares – $\phi \approx$ 0.25

(*a*)

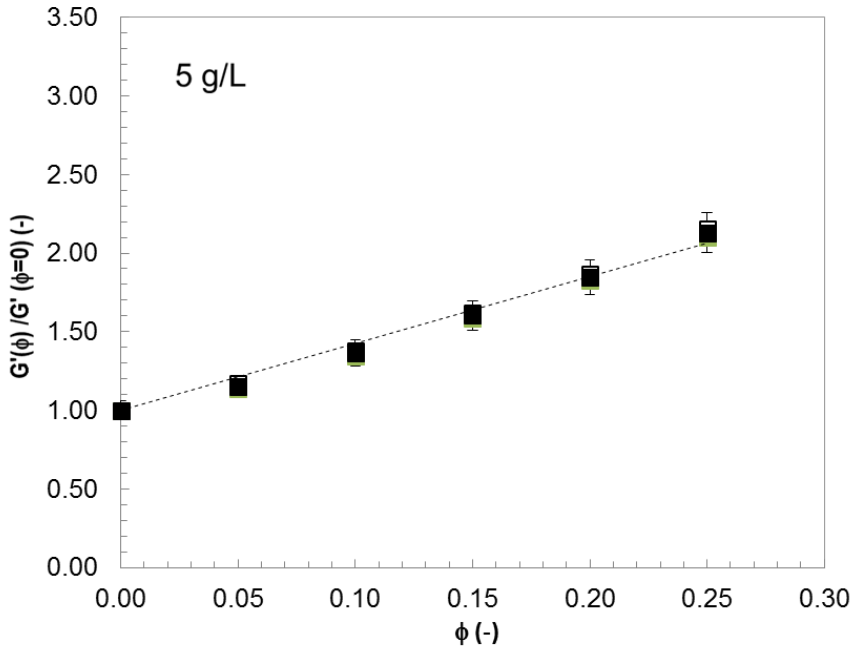

(*b*)

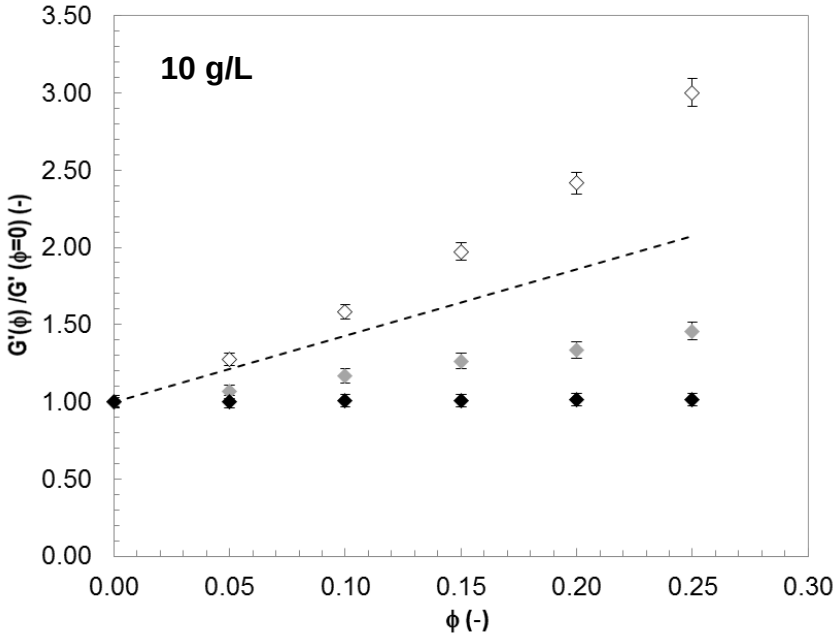

Figure 5 Effect of bubble volume fraction on elastic modulus for bubbly liquids prepared with (*a*) 5 g/L and (*b*) 10 g/L aqueous guar gum solution; (c) phase angle at selected frequencies. Symbols: squares – 5g/L, diamonds – 10 g/L, open – 0.1 Hz, grey – 1 Hz, black – 4 Hz. Dashed line in (*a*) shows fitted linear trend with $G'(\phi)/G'(0) = 1 + 4.3\phi$. Dashed line in (*b*) shows $G'(\phi)/G'(0)$ for bubbly liquids prepared at 5 g/L.

(*c*)

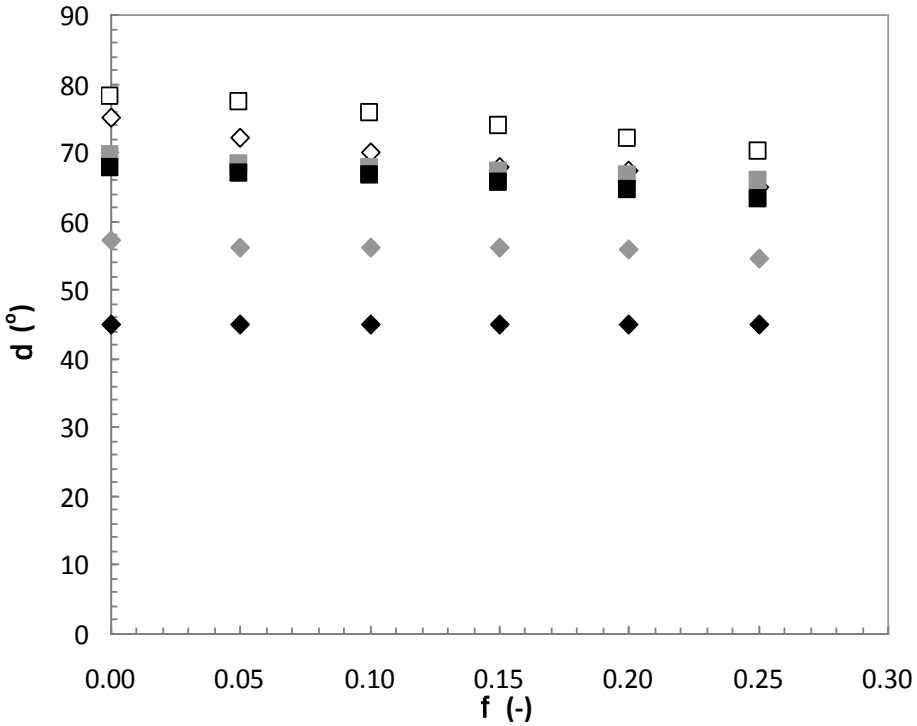

Figure 5 Effect of bubble volume fraction on elastic modulus for bubbly liquids prepared with (*a*) 5 g/L and (*b*) 10 g/L aqueous guar gum solution; (c) phase angle at selected frequencies. Symbols: squares – 5g/L, diamonds – 10 g/L, open – 0.1 Hz, grey – 1 Hz, black – 4 Hz. Dashed line in (*a*) shows fitted linear trend with $G'(\phi)/G'(0) = 1 + 4.3\phi$. Dashed line in (*b*) shows $G'(\phi)/G'(0)$ for bubbly liquids prepared at 5g/L.

888 (a)

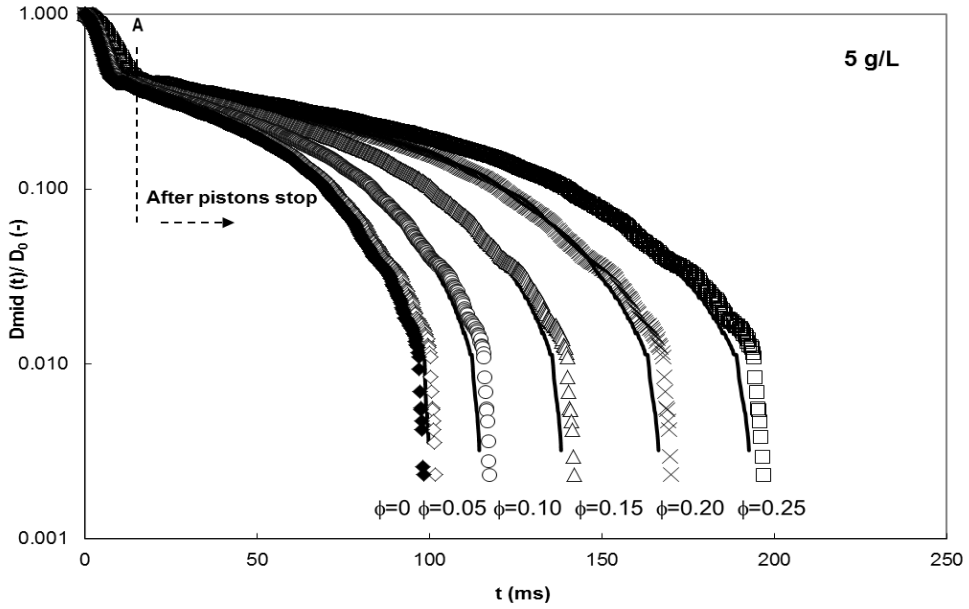

889

890 (*b*)

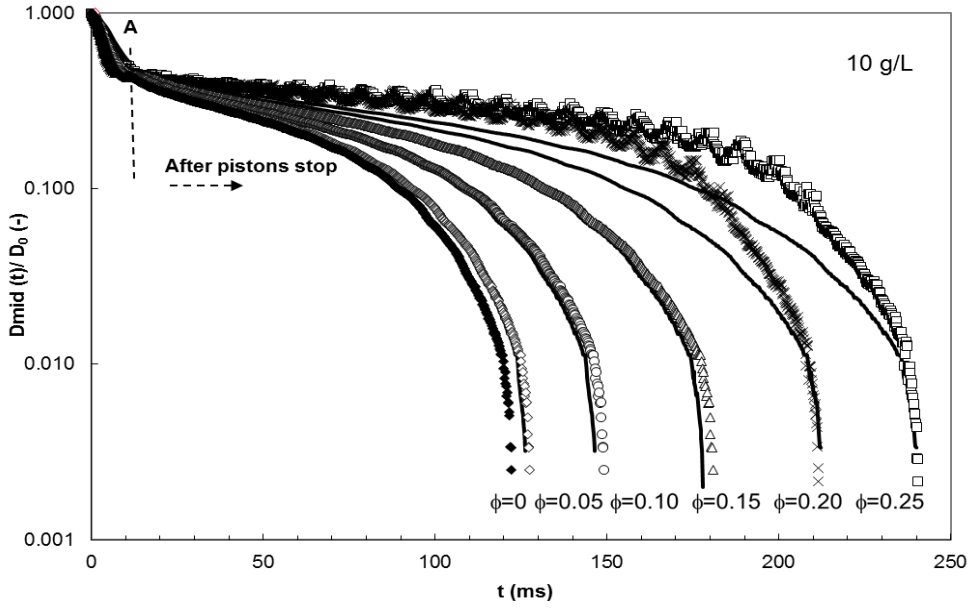

891

892 **Figure 6** Effect of air volume fraction on evolution of dimensionless filament diameter for aqueous
893 guar gum solutions prepared at (*a*) 5 g/L and (*b*) 10 g/L. Symbols: solid diamonds - $\phi \approx$
894 0.00, open diamonds – $\phi \approx$ 0.05, circles - $\phi \approx$ 0.10, triangles – $\phi \approx$ 0.15, crosses – $\phi \approx$
895 0.20, squares – $\phi \approx$ 0.25. Solid lines show experimental data obtained after syringing of the
896 samples. The non-linear profiles indicate non-Newtonian behaviour.

897

(*a*)

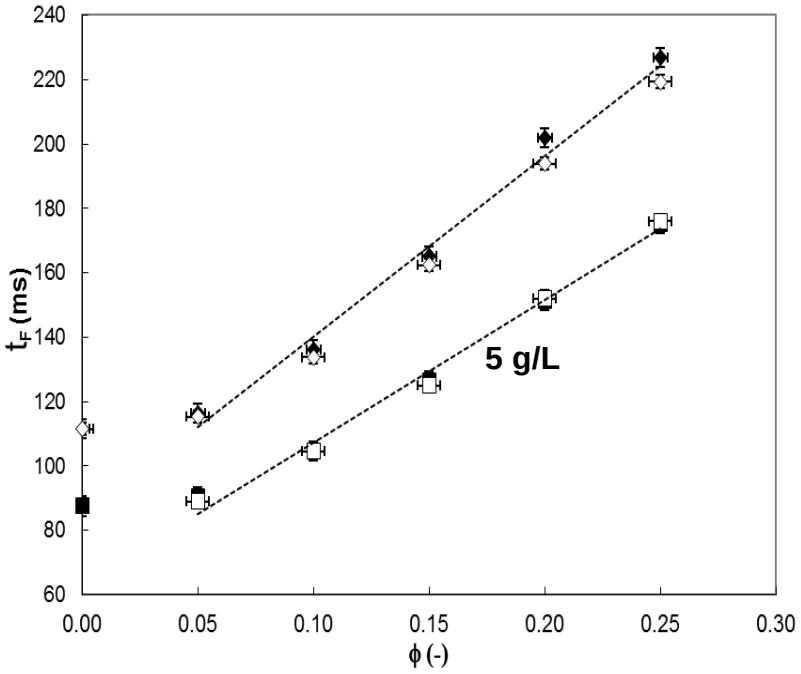

(b)

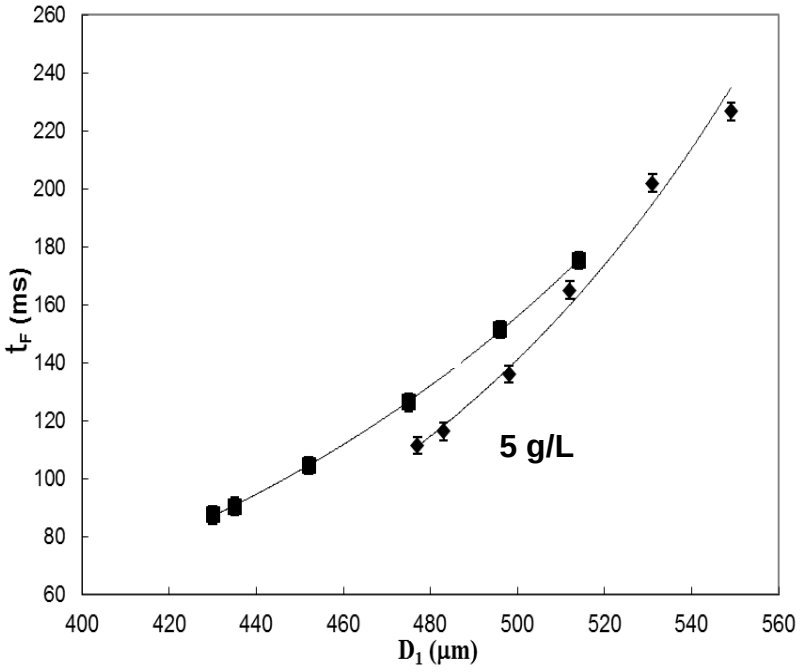

Figure 7 Influence of (*a*) air volume fraction, ϕ, and (*b*) initial filament diameter (D_1) on filament break-up time (t_F). Symbols: diamonds – 10 g/L, squares – 5 g/L. Open symbols show trends obtained after syringing of the samples. Dashed lines show fitted trend lines, Eqns. [13, 14], solid trend lines show Eqns. [15, 16].

907 (*a*)

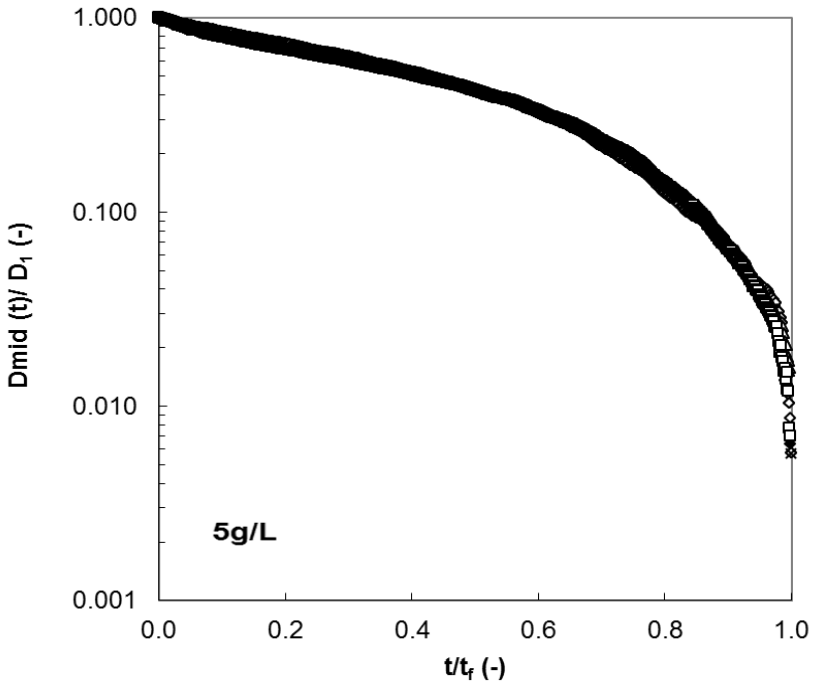

908

909 (*b*)

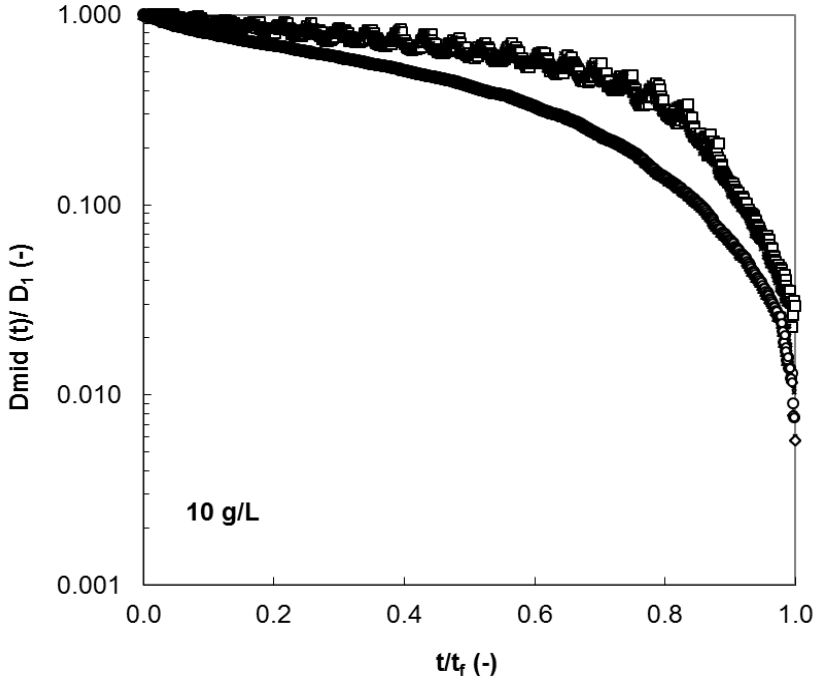

910

911 **Figure 8** Dimensionless filament diameter - dimensionless time profiles for aqueous guar gum
912 solutions prepared at (*a*) 5 g/L and (*b*) 10 g/L. Symbols: solid diamonds - $\phi \approx 0.00$,
913 diamonds – $\phi \approx 0.05$, circles - $\phi \approx 0.10$, triangles – $\phi \approx 0.15$, crosses – $\phi \approx 0.20$, squares –
914 $\phi \approx 0.25$.

915 (*a*)

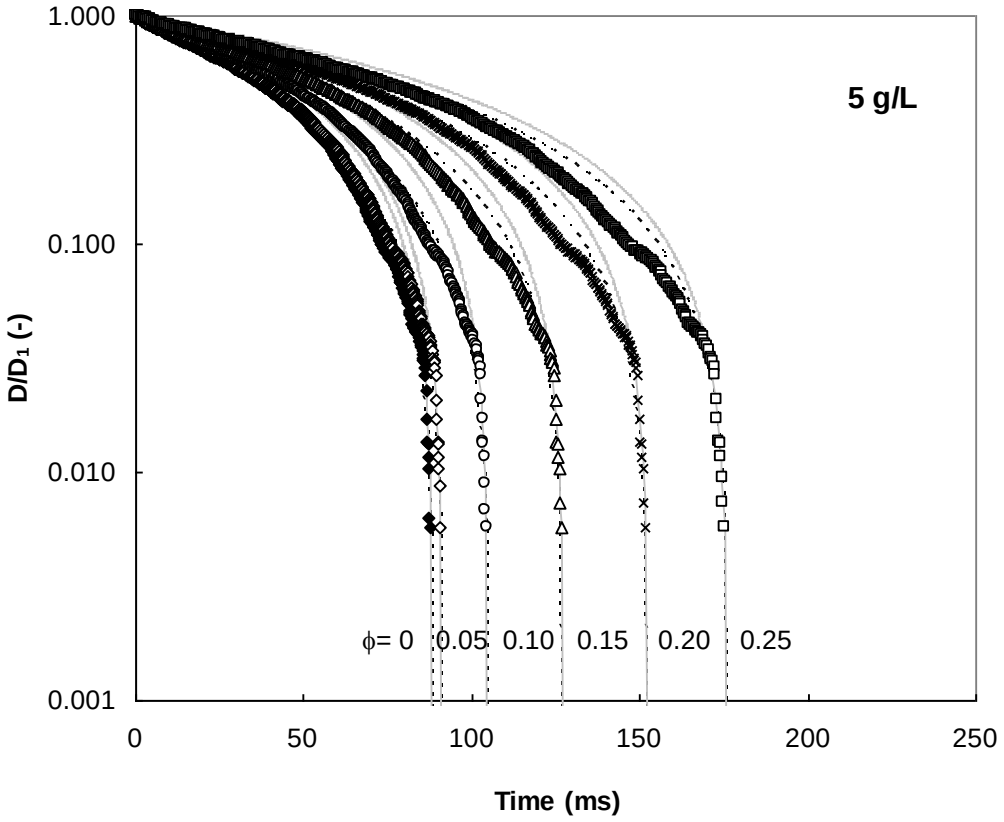

916

917 (*b*)

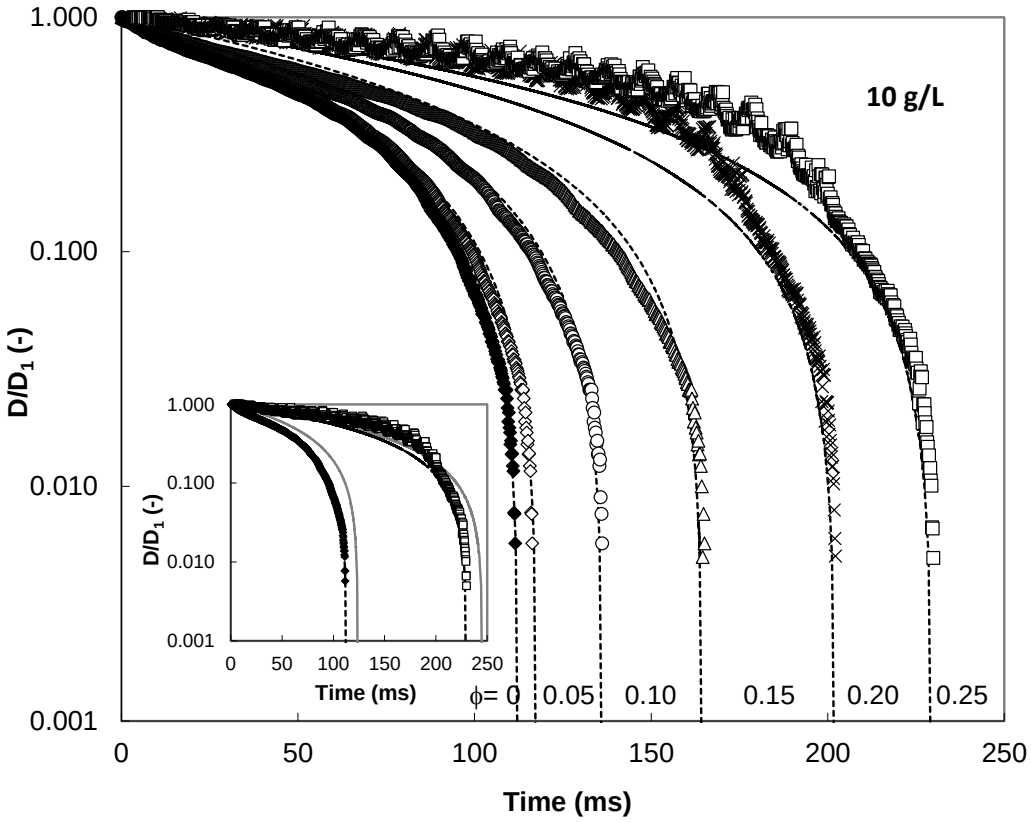

918

(*c*)

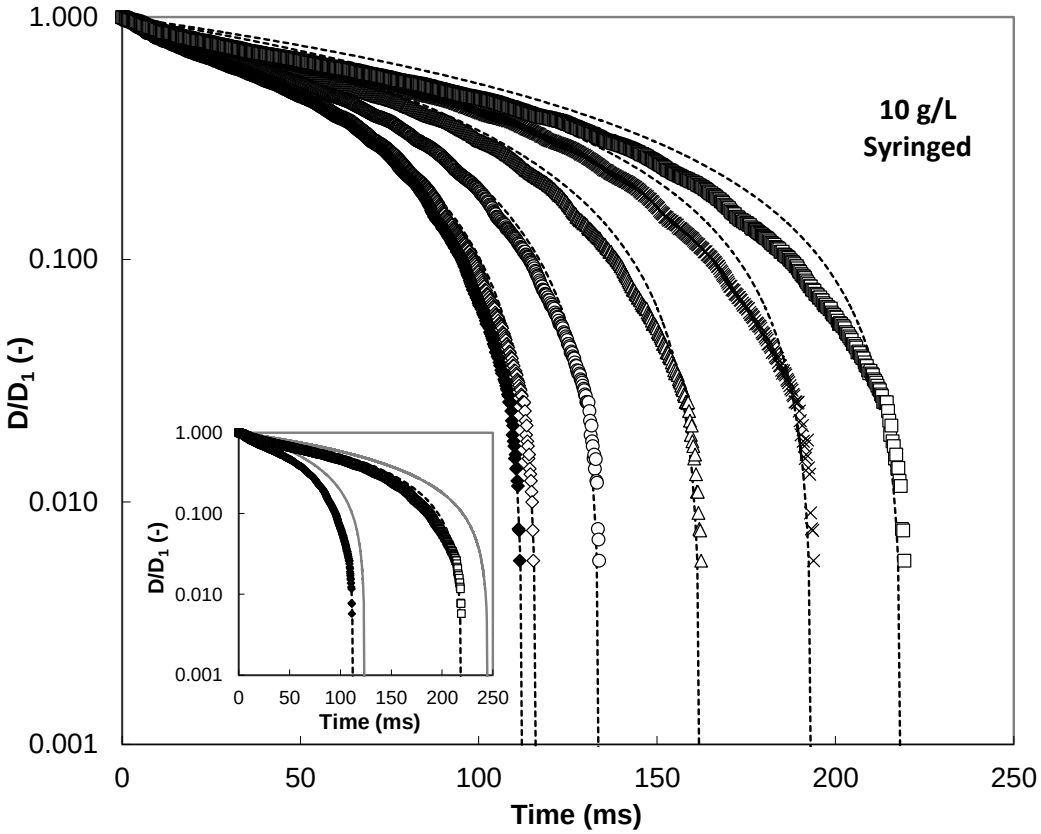

Figure 9 Comparison of measured non-dimensional filament diameter with Giesekus model, Equation [11] for selected aqueous guar gum solutions prepared at (*a*) 5 g/L, (*b*) 10 g/L and (*c*) 10 g/L after syringing. Symbols: solid diamonds - $\phi \approx 0.00$, diamonds – $\phi \approx 0.05$, circles - $\phi \approx 0.10$, triangles – $\phi \approx 0.15$, crosses – $\phi \approx 0.20$, squares – $\phi \approx 0.25$. Solid loci in (*a*) show Equation [11] where parameters a and λ are those obtained from fitting both linear shear and extensional data, Table 2. Dashed loci show Equation [11] with parameters obtained by fitting to extensional data alone (Table 2 and Table 3).

(*a*)

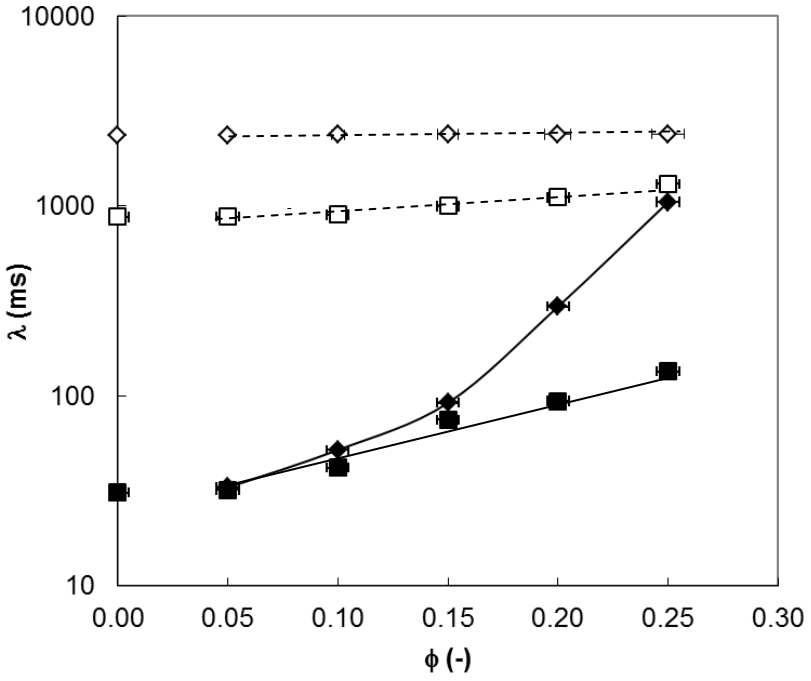

(*b*)

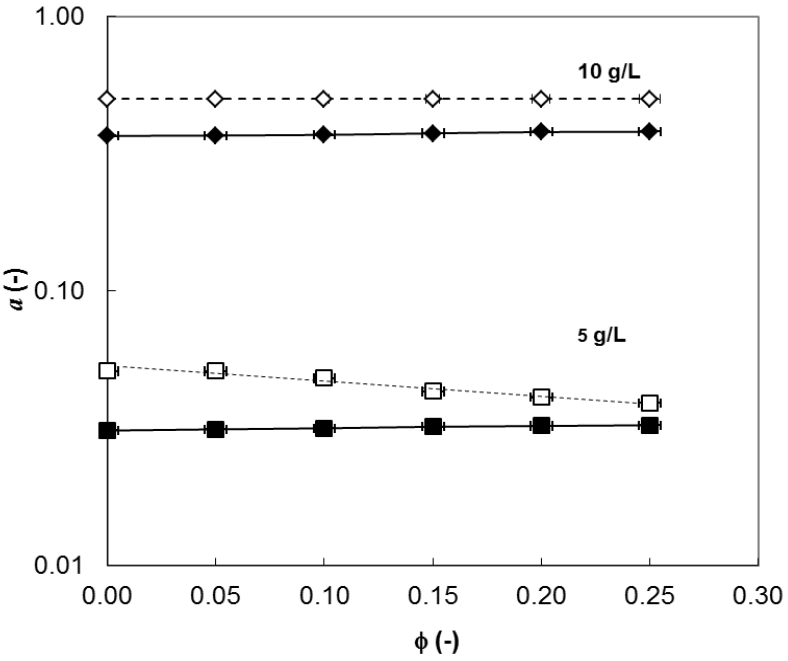

Figure 10 Effect of air volume fraction on Giesekus model parameters: (*a*) relaxation time, λ, and (*b*) mobility parameter, *a*. Symbols: squares – 5 g/L, diamonds – 10 g/L. Open symbols, dashed lines – fitted to linear shear alone; solid symbols, solid lines – fitted to extensional data alone.

(*a*)

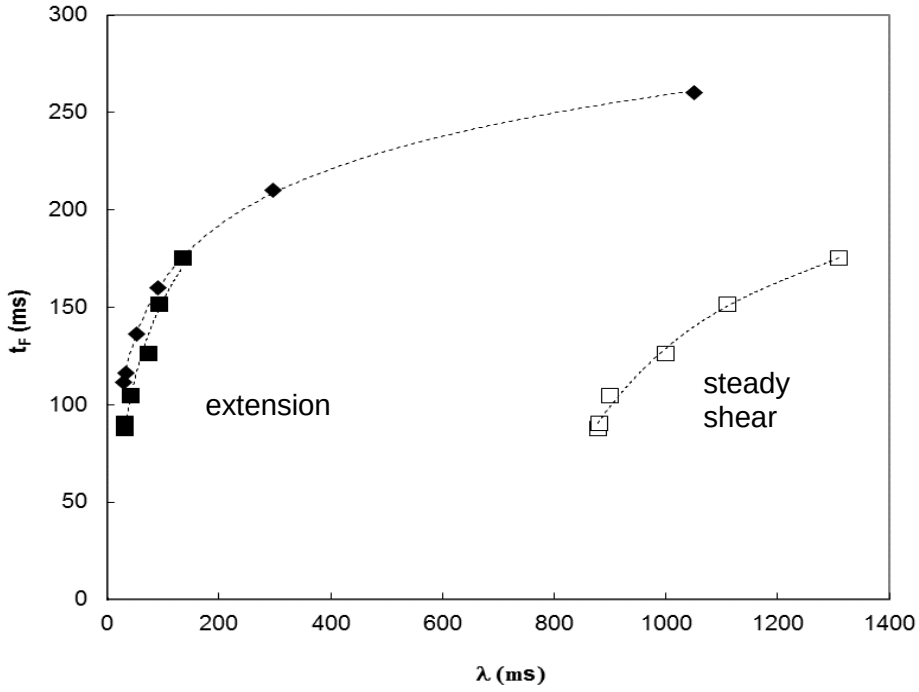

(*b*)

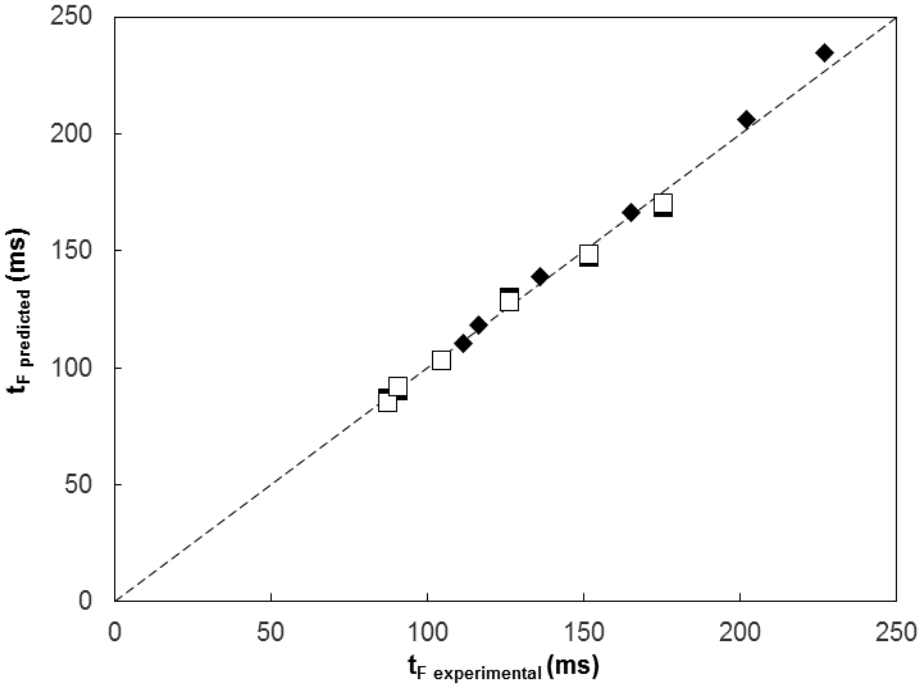

Figure 11 Correlation between (*a*) measured filament break-up time (t_F) and estimated relaxation time for guar gum bubbly liquids at different air volume fractions. (*b*) Comparison between experimental and predicted break-up times. Symbols: squares – 5 g/L, diamonds – 10 g/L. Open symbols denote 5 g/L data sets where the Giesekus parameters were obtained from steady shear measurements.

(*a*)

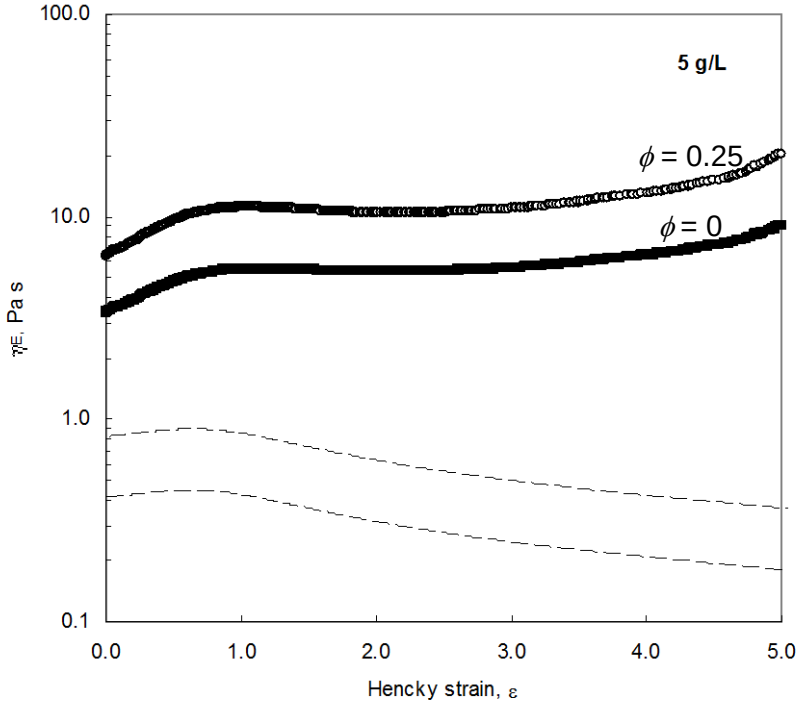

(*b*)

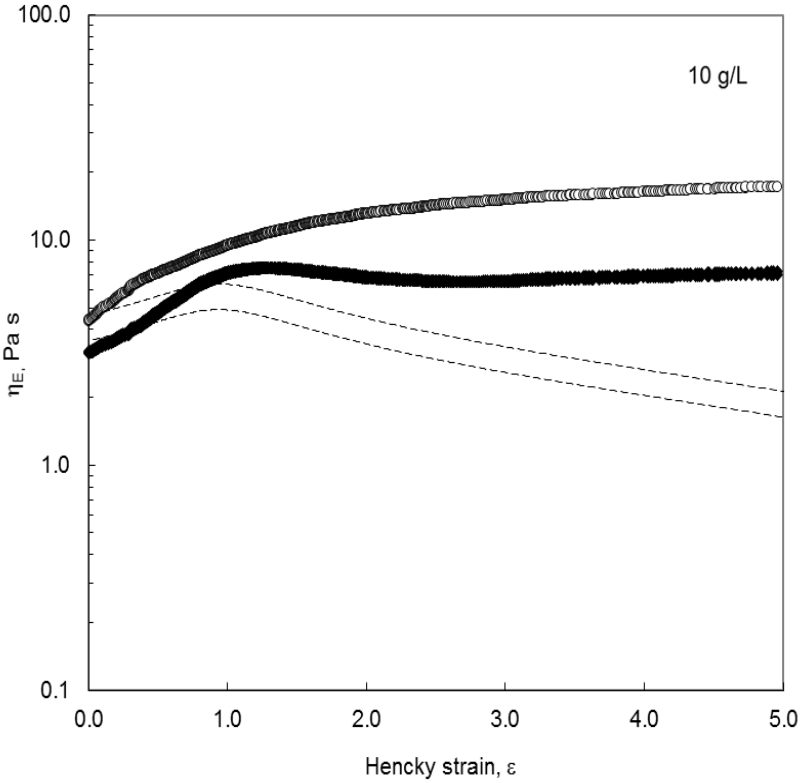

Figure 12 Effect of Hencky strain on apparent extensional viscosity of bubbly liquids generated by 10 min aeration ($\phi \approx 0.25$) of guar gum solutions at (*a*) 5 g/L and *(b)* 10 g/L. Solid symbols – $\phi \approx 0.00$, open symbols – $\phi \approx 0.25$. Dashed lines show the prediction for extension of a Cross model fluid estimated using Equation [20].

Table Captions

Table 1 Log-normal† bubble size distribution parameters for bubbly liquids prepared with aqueous guar gum solutions.

Table 2 Parameters obtained by fitting the steady shear and extensional data for 5 g/L guar gum solutions and bubbly liquids to Equation [5] and Equation [11], and to filament stretching (Figure 9) alone.

Table 3 Summary of parameters obtained by fitting data from 10 g/L guar gum to Equation [6] for linear shear (Figure 2) and Equation [11] for extensional shear (Figure 9).

964 **Table 1** Log-normal[†] bubble size distribution parameters for bubbly liquids prepared with aqueous guar gum solutions.[*]
965

Solution	5 g/L				10 g/L			
	Without syringing		*With syringing*		Without syringing		*With syringing*	
ϕ (–)	ln μ	ln σ	ln μ	ln σ	ln μ	ln σ	ln μ	ln σ
0.00	-	-	-	-	-	-	-	-
0.05	4.84±0.02[a]	-0.17±0.03[e]	*3.98±0.04[a]*	*-0.39±0.01[e]*	4.84±0.02[a]	-0.073±0.003[e]	*4.03±0.02[a]*	*-0.31±0.01[e]*
0.10	4.79±0.03[a,b]	-0.30±0.02[d]	*3.76±0.03[a]*	*-0.43±0.01[d]*	4.79±0.02[a]	-0.17±0.02[d]	*3.81±0.04[a]*	*-0.34±0.01[d]*
0.15	4.75±0.01[b]	-0.43±0.01[c]	*3.54±0.02[b]*	*-0.46±0.01[c]*	4.72±0.01[b]	-0.30±0.02[c]	*3.59±0.01[b]*	*-0.39±0.02[c]*
0.20	4.72±0.01[b]	-0.58±0.03[b]	*3.52±0.01[b]*	*-0.54±0.02[b]*	4.70±0.01[b]	-0.43±0.01[b]	*3.58±0.01[b]*	*-0.46±0.02[b]*
0.25	4.71±0.01[b]	-0.69±0.02[a]	*3.49±0.01[b]*	*-0.63±0.02[a]*	4.64±0.02[b]	-0.54±0.03[a]	*3.54±0.01[b]*	*-0.53±0.02[a]*

966 [*]Data are presented as mean ± standard deviation. Data values in a column with different superscript letters are significantly different at the $p \leq 0.05$ level.

967 [†]Log-normal distribution equation is $f(x;\mu,\sigma) = \frac{1}{x\sigma\sqrt{2\pi}} e^{-\frac{(\ln x-\mu)^2}{2\sigma^2}}$, where x is the studied variable, μ, the mean and σ the standard deviation.

968

Table 2 Parameters obtained by fitting the steady shear and extensional data for 5 g/L guar gum solutions and bubbly liquids to Equation [5] and Equation [11], and to filament stretching (Figure 9) alone.

					Linear and extensional shear Equation [5, 11]			Extensional shear alone Equation [11]		
ϕ (–)	[a] D_1 (μm)	[a] α (N/m)	[a] $\eta_{0,\,exp}$ (Pa s)	[b] $\eta_{0,\,cal}$ (Pa s)	[b] a (-)	[b] λ (s)	R^2	[b] a (-)	[b] λ (s)	R^2
0.00	430	0.0675	0.48	0.48	0.051	0.878	0.993	0.0312	0.029	0.995
0.05	435	0.0675	0.50	0.49	0.051	0.880	0.982	0.0314	0.030	0.992
0.10	452	0.0675	0.52	0.50	0.048	0.900	0.983	0.0317	0.041	0.994
0.15	475	0.0675	0.55	0.54	0.043	1.00	0.980	0.0324	0.073	0.989
0.20	496	0.0675	0.60	0.57	0.041	1.11	0.980	0.0324	0.091	0.986
0.25	514	0.0675	0.65	0.60	0.039	1.31	0.979	0.0326	0.133	0.982

[a]Measured parameters

[b]Fitted parameters

974 **Table 3** Summary of parameters obtained by fitting data from 10 g/L guar gum to
975 Equation [6] for linear shear (Figure 2) and Equation [11] for extensional shear (Figure 9).
976

					Linear shear			Extensional shear		
ϕ (–)	[a]D_1 (μm)	[a]α (N/m)	[a]$\eta_{0,\,exp}$ (Pa s)	[b]$\eta_{0,\,cal}$ (Pa s)	[b]a (-)	[b]λ (s)	R^2	[b]a (-)	[b]λ (s)	R^2
Without syringing										
0	477	0.0674	5.90	5.87	0.5	2.365	0.950	0.467	0.023	0.967
0.05	483	0.0674	5.95	5.94	0.5	2.372	0.779	0.468	0.029	0.994
0.10	498	0.0674	6.15	6.11	0.5	2.381	0.764	0.470	0.048	0.992
0.15	512	0.0674	6.75	6.68	0.5	2.393	0.763	0.475	0.087	0.991
0.20	531	0.0674	7.20	7.05	0.5	2.395	0.762	0.478	0.292	0.955
0.25	549	0.0674	7.50	7.34	0.5	2.396	0.760	0.481	1.045	0.943
With syringing										
0	477	0.0674	5.90	5.87	0.5	2.365	0.955	0.467	0.023	0.997
0.05	480	0.0674	5.95	5.92	0.5	2.372	0.754	0.468	0.030	0.994
0.10	491	0.0674	6.10	6.07	0.5	2.381	0.742	0.470	0.049	0.995
0.15	508	0.0674	6.70	6.62	0.5	2.393	0.740	0.475	0.087	0.992
0.20	518	0.0674	7.10	6.99	0.5	2.395	0.741	0.479	0.241	0.991
0.25	542	0.0674	7.40	7.28	0.5	2.396	0.742	0.480	0.490	0.984

977 [a]Measured parameters

978 [b]Fitted parameters
979

980

ϕ = 0.25

ϕ = 0

Table A.1 Parameter values obtained for Cross-Williamson model, Equation [A.1], for whisked aqueous guar gum solutions prepared at several air volume fractions. †

	ϕ (–)	η_0 (Pa s)	k (s $^{1-n}$)	n (-)	R^2	s (Pa s)
5 g/L	0.00	0.48±0.01^{d,e}	0.19±0.01^{c}	0.30±0.00^{a}	0.998	0.027
	0.05	0.50±0.0^{d}	0.21±0.01^{b,c}	0.30±0.01^{a}	0.999	0.026
	0.10	0.52±0.01^{d}	0.23±0.01^{b}	0.30±0.01^{a}	0.999	0.023
	0.15	0.55±0.01^{c}	0.24±0.01^{a,b}	0.29±0.01^{a,b}	0.998	0.028
	0.20	0.60±0.01^{b}	0.25±0.01^{a}	0.28±0.00^{b}	0.999	0.024
	0.25	0.65±0.02^{a}	0.26±0.01^{a}	0.28±0.00^{b}	0.997	0.031
10 g/L	0.00	5.90±0.01^{d,e}	0.61±0.01^{c}	0.32±0.00^{a}	0.997	0.028
	0.05	5.95±0.02^{d,e}	0.62±0.01^{b,c}	0.32±0.01^{a}	0.999	0.026
	0.10	6.15±0.01^{d}	0.63±0.01^{b}	0.32±0.01^{a}	0.998	0.027
	0.15	6.75±0.01^{c}	0.64±0.01^{a,b}	0.31±0.01^{a,b}	0.998	0.027
	0.20	7.20±0.01^{b}	0.65±0.01^{a}	0.30±0.00^{b}	0.999	0.025
	0.25	7.50±0.02^{a}	0.67±0.01^{a}	0.30±0.00^{b}	0.997	0.031

†Data are presented as mean ± standard deviation. Data values in a column with different superscript letters are significantly different at the $p \leq 0.05$ level.